Efficiency Optimization of Vector Controlled Induction Motor Drive

DISSERTATION SUBMITTED IN PARTIAL FULFILLMENT OF THE REQUIREMENTS FOR THE AWARD OF THE DEGREE

OF

MASTER OF TECHNOLOGY
IN
CONTROL & INTRUMENTATION

Submitted by:

JALAJ ARORA

(2K14/C&I/21)

Under the Supervision of

Dr. Mini Sreejeth

DEPARTMENT OF ELECTRICAL ENGINEERING

DELHI TECHNOLOGICAL UNIVERSITY
(Formerly Delhi College of Engineering)
Bawana Road, Delhi-110042

2016

DEPARTMENT OF ELECTRICAL ENGINEERING
DELHI TECHNOLOGICAL UNIVERSITY
(Formerly Delhi College of Engineering)
Bawana Road, Delhi-110042

CERTIFICATE

I, **Jalaj Arora**, student of **M. Tech. (C&I)**, 2k14/C&I/21 hereby declare that the thesis titled "Efficiency Optimization of Vector Controlled Induction Motor Drive" has been done under the guidance of Dr. Mini Sreejeth, Assistant Professor, Electrical Engineering Department (EED), Delhi Technological University (DTU) in the partial fulfilment of requirement for the award of the degree of Master of Technology has not been submitted elsewhere for the award of any Degree.

Place: New Delhi **JALAJ ARORA**

Date: 18.07.2016

Dr. Mini Sreejeth
Assistant Professor
Department of Electrical Engineering (EED)
Delhi Technological University (DTU)

ACKNOWLEDGEMENT

It is a genuine pleasure to express my deep sense of thanks and gratitude to my mentor, philosopher and guide Dr. Mini Sreejeth. Her dedication and keen interest above all her overwhelming attitude to help her students had been solely and mainly responsible for completing my work. Her timely advice, meticulous scrutiny, scholarly advice and scientific approach have helped me to a very great extent to accomplish my thesis "Efficiency optimization of Induction motor".

I owe a deep sense of gratitude to Dr. Madhusudan Singh, Head of Department and faculty members of Electrical Engineering Department for their keen interest on me at every stage of my research. Their prompt inspirations, timely suggestions with kindness, enthusiasm and dynamism have enabled me to complete my thesis.

I thank profusely all the STAFFs of electrical department laboratories for their kind help and co-operation throughout my study period.

I am extremely thankful to all my classmates, friends for providing me necessary technical suggestions during my research pursuit.

JALAJ ARORA

ABSTRACT

Induction motors are widely used in domestic, commercial and industrial application. About 80% of the auxiliaries used in thermal power plant are induction motors. And, in households almost all rotating machines are induction motors. Most of the applications of induction motors (IMs) are based on variation in speed according to the load demand. Induction machines are non linear machines and there exist high dynamic interactions. Hence, in order to emulate it as separately excited DC motor, vector control technique is used as this method removes the coupling effects (using a frame of reference like synchronous, stationary) which makes the response sluggish. Traditionally, PI controllers are generally used in order to control the speed but tuning is somewhat time consuming as values have to be changed every time when parameters are changed. In order to avoid this fuzzy controllers are used. Also, induction motors consume a major part of the total electrical energy production. Therefore, improving the efficiency of the induction motor is always been a major concern. Various essential strategies are adopted to ensure optimum efficiency operation of induction motor drive. This is usually realized either by selecting proper control strategies or by improvement in the design, materials and construction techniques or both. Design aspects involve shaping of rotor bars, use of copper material instead of aluminium, etc. The control strategies adopted to optimize the efficiency are search controller and loss model controller. Search controller method is a feedback method that finds maximum efficiency by adopting a search technique. The value of efficiency at a particular sampling instant is compared with the efficiency value of previous sampling instant and necessary control action is executed accordingly. Loss model controller depends on motor parameters because it is based on the modelling of the motor and losses to derive an objective function, which is optimized to yield maximum efficiency. Machines are designed to operate at rated flux because if gives fast transient response and high torque to ampere ratio. If rated flux is maintained at light loads, then core losses of the machine will be excessively high which will result in reduced efficiency. Here, loss model control technique will be used to reduce the losses and increase the torque per ampere ratio by making rated flux as increasing function of load.

TABLE OF CONTENTS

LIST OF FIGURES

LIST OF TABLES

ABBREVIATIONS USED IN THESIS

R_s	Resistance of stator (Ω)
R_r	Resistance of rotor (Ω)
Ψ_{ds}	d^e axis flux linkage on stator (Wb)
Ψ_{qs}	q^e axis flux linkage on stator (Wb)
L_m	Mutual inductance of machine (H)
i_{ds}	d^e axis current on stator (A)
i_{qs}	q^e axis current on stator (A)
Ψ_{dr}	d^e axis flux linkage on rotor (Wb)
Ψ_{qr}	q^e axis flux linkage on rotor (Wb)
i_{dr}	d^e axis current on rotor (A)
i_{qr}	q^e axis current on rotor (A)
L_s	Self-inductance of stator (H)
L_r	Self-inductance of rotor (H)
L_{ls}	Leakage inductance of stator (H)
L_{lr}	Leakage inductance of rotor (H)
Ψ_{dm}	d^eaxis magnetizing flux linkage (Wb)
Ψ_{qm}	q^eaxis magnetizing flux linkage (Wb)
T_e	Electromagnetic Torque of machine (Nm)
T_L	Load Torque (Nm)
ω_m	Speed of the motor in mechanical rad/s
ω_e	Synchronous speed in electrical rad/s
J	Motor Inertia
P	Pole pairs

CHAPTER 1

INTRODUCTION

1.1 General

Induction motor drive is the integral part of the electrical drives that is used in various manufacturing process. It is widely used in industries for position, speed and torque control applications because of its structure, ruggedness, high reliability, robustness, efficiency, high reliability and cost. Further, to achieve higher productivity and product quality, automated control and continuous monitoring of these drives can also be done. Few decades back, speed control of induction motor with high performance is somewhat difficult but with the introduction of power electronics, various control techniques has been developed to make use of induction motor to large extend in many applications[1,2]. Control of induction motor is a tough task as compared to DC motor because in order to control torque, access to rotor quantities is necessary which is not easy. If the components of stator current i.e. flux and torque get supply from a controlled source, the dynamics of induction motor can be compared to the DC motor[3].

Electrical energy plays a vital role in day to day life. In few decades, the growth of manufacturing industries has been tremendously increased, which in turn mounted the demand of electrical energy. Hence, reducing the energy utilization has drawn the industrial attention to the losses and efficiency of the motors and overall drive system. This will help in judicious use of natural resources, reducing the adverse effects on environment and cutting the cost of electricity bills to stimulate the economy of industries. Efficiency optimization technique has been implemented on induction motor drives and results are compared against conventional method. After applying the above technique, its impact on motor losses, parameters and other variables have also been analysed using sensitivity analysis.

1.2 Electrical Drives Control and Monitoring

In large industries, there are several electrical drives located at various positions according to its applications and mode of operation. Hence, the monitoring of these drives is of utmost importance.

1.3 Organisation of Thesis

This thesis reveals the performance parameters, control methods and operation of Induction motor drive. Different control techniques with different controllers are implemented and also demonstrated on the drive and results are studied and analysed in MATLAB Simulink environment. Also, the effect of efficiency optimization methods on dynamic and steady state performance of the drive is also analysed and results of drive using different controllers are compared. The research work done on concerned topic is as follows:

- Chapter 2: Literature Review

  This chapter includes study of various research papers of the concerned field that is published in IEEE Transactions, IEEE international conferences and other journals.

- Chapter 3: Dynamic Model of Induction Motor

  In this chapter, dynamic modelling of induction motor is carried out, where the axes transformations like Clarke's transformation and Park's transformation is also analysed. To eliminate all time varying inductance appearing in the equations, a synchronously rotating reference frame is used in the modelling of induction motor.

- Chapter 4: Techniques to Control Induction Motor

  This chapter introduce different techniques (i.e. scalar control, indirect and direct vector control, sensor-less control and direct vector control) to control the induction motor. With the introduction of power electronics and intelligent control methods like Fuzzy Logic controller, such control techniques are possible.

- Chapter 5: Efficiency Optimization of Three Phase Induction Motor

  This chapter includes efficiency optimization algorithm for indirect vector controlled induction motor to reduce overall losses. This efficiency optimization control algorithm optimizes the d – axis current to minimize the controllable electrical losses for a given torque and speed. Their mathematical derivation and

MATLAB Simulink results under different operating conditions like change in speed, load etc. are evolved.

- Chapter 6: Simulation results of Efficiency Optimization of Three Phase Induction Motor
  This chapter introduces modelling, simulation and analysis of indirect vector controlled induction motor drive. Also, efficiency optimization control algorithm has been developed and modelled in MATLAB Simulink and performance of the motor under dynamic conditions is analysed in detail. The algorithm optimizes the d – axis current component and minimizes the controllable electrical loss for a given torque and speed. The performance of the drive with and without algorithm has been validated through mathematical derivation and simulation results under dynamic conditions like sudden change in speed, load etc. The efficiency optimization control algorithm significantly minimizes the losses and improves the efficiency of the drive at low load conditions as compared to conventional constant flux method. But, dynamic response is good in case of conventional method when compared with implemented efficiency optimization control algorithm.

- Conclusion and Future Scope
  This chapter concludes the comparison studies of efficiency optimization technique applied to indirect vector control using two different controllers i.e. Hysteresis current controller and SVPWM (Space Vector Pulse Width Modulation) and also same comparison have been done without using efficiency optimization technique i.e. conventional method. Finally, a comprehensive account of suggestions for further extension of this research work which is feasible is presented.

1.4 Conclusion

This chapter provides an overview of research work carried out and also the objectives and research work carried out.

CHAPTER 2

LITERATURE REVIEW

2.1 General

Induction motor drives are widely used in industries for various applications because of their high torque to weight ratio as compared to DC motor, robust structure, sustainable to operate in hazardous place. However, due to their complex and nonlinear structure, control of induction motor is a challenging task. The main reason behind this complexity is requirement of variable frequency, harmonically optimum converter power supplies, Complex dynamic of ac machines, and variation in machine parameters. In recent years due to advancement in technology of power electronics and introduction of various control schemes which makes induction motor drive suitable for various industries as for industrial purpose the dynamic performance of the induction motor drive must have good dynamic performance. Also, power electronics devices has also become sophisticated in few decades that is attracting various industries to use this in drives. In this chapter the various research on modelling of induction motor and its control strategies are discussed. This chapter mainly includes field oriented control strategy with efficiency optimization for induction motor drive.

2.2 Modelling And Control of Induction Motor Drive

Induction motor drive is widely used in the industries and power plants as auxiliary machine for carrying out various tasks like moving of coal etc. because of its versatile performance characteristics. An Intel 8051, 8 bit microcontroller can be used to generate pulses required for 3 phase inverter as this microcontroller has separate time based register that can produce accurate delays required for pulses. This is reported by Varnovitsky [26]. The characteristics and performance of induction motor drive using power electronics devices is used for variable frequency operation is investigated by Barnes [27]. Current Source inverter fed induction motor in which output current level remain constant without using free-wheeling diodes and voltage source fed induction motor where output voltage remain constant are reported by R. Krishnan [28]. Intel 8086, 16 bit microprocessor can also produce six pulses of variable frequency required for 3 phase inverter using simple assembly language. This is used to control induction motor that exhibit magnetic saturation because of economic reasons modern machines are designed to operate at saturation [29].

2.2.1 Controlling Techniques

Over the last three to four decades the improvement in dynamic performance of induction motor drive is always major concern among researchers, as engineers of industries were constantly facing problems because of induction motor performance characteristics. Hence, many control schemes have been emerged such as direct torque control, sensor less control, vector or field oriented control of induction motor drive.

In 1968, FOC (Field oriented control) scheme was developed in Germany. Blaschke proposed direct vector control technique and Hasse proposed indirect vector control that created a new revolution in field of drives. Later, Field oriented schemes were introduced by Werner Leonhard for dynamic performance [5] [6] [7]. Esmaily et al. [4] wrote an article in which uniform pulse width modulation technique is used for vector control scheme in induction motor drives. Hasan Zidan et al. [8] investigated a speed estimation method for induction motor drive operating at low speeds, which uses input voltage and currents in closed loop for rotor parameter estimation. A. Munoz –Garcia et al. [10] presents a novel on open-loop speed control method for induction motors that provides high output torque and nearly zero steady-state speed error at any frequency. The control scheme used is based on constant volts per hertz (V/f) method using low-cost open-loop current sensors. The scheme proposed fully compensates for the current-resistance (IR) voltage drop by vectorially modifying the stator voltage and keeping the magnitude of the stator flux constant, regardless of changes in frequency or load. Jee Hoon Jung et al. [12] proposed a scheme to improve the stability of V/f-controlled induction motor drive systems by a dynamic current compensator. The proposed method uses a dynamic current compensator to improve the stability of the V/f-controlled induction motor drive systems. This method is easy to implement and helps eliminate the oscillations causing the instability of V/f-controlled induction motor drive systems. Mohamed S. Zaky et al. [13] proposed a parallel identification schemes for both speed and stator resistance of sensorless induction motor drives for a wide range of speed estimation. These estimation algorithms combine a sliding-mode current observer with Popov's hyperstability theory. Low- and zero-speed operations of the proposed sliding-mode-observer (SMO)-based speed estimation combined with an online stator resistance adaptation scheme are also investigated. A modified SMO-based speed estimation scheme for field-weakening operation is also introduced. J. Guzinski et al.[14] presented a low-cost implementation of the sensorless vector control of an induction motor. The system is based on a new set of variables for the induction motor model and works by using vectors coordinates in a stationary α-β frame of references. A phase-locked loop was used to control the angle between the flux vector and the stator current vector. A current controller for the current-regulated pulse width-modulation inverter based on the simplified load model is used. H.M. Kojabadi et al. [15] presents a paper which provides a novel method of estimating both the shaft speed and stator resistance of an induction motor. In this novel scheme, an adaptive pseudo reduced-order flux observer (APFO) is developed. In comparison to the adaptive full-order flux observer (AFFO), the proposed method consumes less computational time, and provides a better stator resistance estimation dynamic performance. Gianmario Pellegrino et al. [16] presents a simple and accurate method for the identification of inverter parameters at the drive startup. The method is integrated into the control code of the IM drive, and it is based on the information contained in the feedback signal of the flux observer. The procedure applies to all those sensorless ac drives where the flux is estimated using the back-EMF integration. H. Benderradji et al. [17] presents a paper that deals with the control and observation of an induction motor using second order sliding-mode technique and a new Lyapunov function for the stability analysis. This approach guarantees the same robustness and dynamic performance of traditional first-order SMC algorithms, and at the same time, attenuates the chattering phenomenon. F. – J. Lin. et al. [18] presents an adaptive back stepping sliding mode controller, which combines both the merits of adaptive back stepping control and sliding mode control which will control the mover position of a linear induction motor (LIM) drive to compensate for the uncertainties including the friction force. First, the dynamic model of an indirect field-oriented LIM drive is derived, then, a back stepping sliding mode approach is proposed to compensate the uncertainties which occur in the motion control system. Min-Ho-Park et al. [19] showed that in a sliding mode control, the control function is discontinuous on the hyperplane, which causes harmful effects such as current harmonics and acoustic noise in the motor drive application. Hence, a low-pass filter is introduced between the sliding mode controller output and the motor controller input to reduce these effects.

S. Xepapas et al. [20] proposed a sliding-mode observer for the speed-sensorless direct torque vector control of induction motors is proposed. The observer estimates the motor speed, the rotor flux, the angular position of the rotor flux and the motor torque from measured terminal voltages and currents. The use of the nonlinear sliding-mode technique provides very good performance for both low- and high-speed motor operation and robustness in motor losses and load variations.

M. Cirrincione et al. [21] presents a paper on a new model reference adaptive system (MRAS) speed observer for high-performance field-oriented control induction motor drives based on adaptive linear neural networks. This new MRAS speed observer uses the current model as an adaptive model discretized with the modified Euler integration method. A linear neural network has been then designed and trained online by means of an ordinary least-squares (OLS) algorithm. Yaman B. Zbede et al. [22] presents a novel predictive model reference adaptive system (MRAS) speed estimator for sensorless induction motor (IM) drives applications. The proposed estimator is based on the finite control set-model predictive control (FCS-MPC) principle. The rotor position is calculated using a search-based optimization algorithm which ensures a minimum speed tuning error signal at each sampling period. This eliminates the need for a proportional-integral (PI) controller which is conventionally employed in the adaption mechanism of MRAS estimators. Toshiyuki Irisa et al. [23] investigated the parameter characteristics of different types of IM based on the rotor slot structure namely the enclosed slot and open slot types. An EKF algorithm is used for the identification of rotor flux and the estimation of electrical parameters of the IM by Vicente Leite [24,25].

Yang Wenqiang et al. reported vector control of induction motor using reduced order EKF for the estimation of rotor speed and rotor flux [32].

The stator resistance is also identified to estimate the speed accurately at low speed operation. Min-Huei Kim et al. [35], presented a vector controlled MRAS sensor-less induction motor drive. Adaptive systems consists of various controllers that can be used in the control systems. But, the artificial intelligent controllers provides good control as they are reluctant to parametric variations and provide optimize results that will increase the overall performance of the system. Artificial intelligent systems consists of Fuzzy logic, Neural networks, genetic algorithms. If the system uses more than one intelligent controllers like Neuro-Fuzzy etc then, it is called hybrid controller. On doing so, the system will have the advantages of more than one intelligent controller but at the same time it increases the complexity of the controller because it is somewhat difficult to implement.

Teresa Orlowska et al. [36] presents a paper in which a fuzzy neural network is used as an adaptive speed controller with an extra option for tuning online according to chosen parameters. The neuro fuzzy has some weight that are trained online and speed in error is removed. Fabio Lima et al. [37] developed an Adaptive Neuro Fuzzy Inference System (ANFIS) estimator that is used for speed control of induction motor sensorless drive and that controller replaces the PI controller. In this, ANFIS speed estimator is validated in a magnetizing flux oriented control scheme, but it cannot solve low or zero speed estimation problem. Cerru et al. [38] presented the design and experimental realization of MRAS for indirect field-oriented induction motor drives using fuzzy laws for adaptive process and a neuro fuzzy procedure to optimize the fuzzy rules. Faa-Jeng Lin et al. [52] reported that a real time genetic algorithm for adaptive sliding mode controller that will give optimize values of parameters to yield maximum performance of induction motor drive. M.N. Uddin et al. [39] presents a novel in which fuzzy logic control is used for speed control of induction motor drive. This speed controller is employed in the outer loop and implemented on the DSP board and results are being compared with conventional PI controller at different dynamic operating conditions. B. Karanayil et al. [40] presented a paper in which rotor resistance of induction motor drive using artificial neural networks is energised by fuzzy logic based stator resistance observer. The rotor flux linkages and a voltage model is being compard and error is back propagated to adjust the weights of neural network model for rotor resistance estimation. The stator current and its corresponding estimated value is compared and error is mapped to change in stator resistance with the proposed fuzzy logic.

Yen Shin Lai et al. [11] proposed a hybrid fuzzy controller for direct torque control of induction motor drives. This hybrid fuzzy control law consists of proportional-integral (PI) control at steady state, PI-type fuzzy logic control at transient state, and a simple switching mechanism between steady and transient states, to achieve satisfied performance under steady and transient conditions. The features of the hybrid fuzzy controller are highlighted by comparing the performance of various control approaches, including PI control, PI-type fuzzy logic control (FLC), proportional-derivative (PD) type FLC, and combination of PD-type FLC and I control, for DTC-based induction motor drives. H. Nejjari et al. [9] presented a letter in which a fuzzy logic is applied to induction motor control for condition monitoring. The results of fuzzy logic can be used for accurate induction motors fault diagnosis if the input data are processed in an optimized way. A non linear control strategy is proposed by Damien Grenier et al. [53] for a salient pole permanent magnet synchronous machine which achieves accurate torque control and copper losses minimization without recurring to an internal current loop or to any feed forward compensation. It takes advantage of rotor saliency by allowing direct axis stator current to have non zero values, which in turn improves the power factor of the machine and raises maximum permissible torque. Also, an off-line identification of electrical and mechanical parameters of IMs, using Least Square techniques is discussed by F. Alonge et al. Stator currents, stator voltages and speed are acquired during a start transient and a stop transient. Sensitivity analysis is carried out for the problem of simultaneous estimation of state and parameters for IM controlled in torque and flux by Mazen Alamir. An EKF algorithm is used for the identification of rotor flux and the estimation of electrical parameters of the IM by Vicente Leite Peda V. Medagam et al. reported an EKF based estimation of states and parameters in a sensor less field- oriented three-phase IM with unknown rotor resistance and varying load torque.

The performance of the sensor less vector control depends on the motor parameters which included stator resistance, rotor resistance, stator leakage inductance, rotor leakage inductance and magnetizing inductance, the identification of the parameters is discussed by Jun Zheng et al. The variation of the rotor resistance has great influence on the performance of speed senso less direct torque control system. Chao Zhang et al. proposed an adaptive flux observer for a speed sensor less direct torque controlled IM drive in which the rotor resistance value is updated during operation. In addition, a mathematical model that represents the general frequency characteristics of the rotor bar is proposed by Young-Su Kwon et al. Many estimation techniques used for the vector control of IM fail to track the desired performance due to parameter uncertainties. Therefore an on-line adaption algorithm for parameter identification is necessary. In 2011 Mokhtar Zerikat et al. reported a MRAS-based algorithm for parallel resistance parameters and rotor speed estimation for a sensor-less vector controlled IM.

2.2.2 Efficiency Optimization

As discussed previously, induction motor drives are widely used for various applications in manufacturing plants and other industries. Therefore, efficient utilization of electrical energy is of utmost importance. Various essential strategies are adopted to ensure optimum efficiency operation of induction motor drive. This is usually realised either by selecting proper control strategies or by improvement in the design, materials and construction techniques or both. Design aspects involve shaping of rotor bars, use of copper material instead of aluminium, etc. As copper has high current density and low value of temperature coefficient as compared to aluminium. The control strategies adopted to optimize the efficiency are search controller and loss model controller. Search controller method is a feedback method that finds maximum efficiency by adopting a search technique. The value of efficiency at a particular sampling instant is compared with the efficiency value of previous sampling instant and necessary control action is executed accordingly. Further, back propagation method is also there in search algorithm. In case, the value of efficiency deteriorates in every new sampling instant then controller will back propagate and necessary control action will be taken from that point where efficiency is high. Hence, this method is slow but it is independent of motor parameters. Loss model controller depends on motor parameters because it is based on the modelling of the motor and losses to derive an objective function, which is optimized to yield maximum efficiency. It is a feed-forward method and treats the situation analytically by properly modelling the losses. Hence, this method is fast as compared to search controller.

Mini Sreejeth et al. [41], presented a paper on efficiency optimization of vector controlled three phase induction motor drive. In this paper, loss model controller is used for optimal control of direct axis stator current, which controls the magnitude of flux. Hence, the efficiency of the motor is optimized by weakening the rotor flux, which in turn reduces the core losses. Daniel S. Kirschen et al.[42], reported an adaptive controller implementation for on-line efficiency of a variable frequency induction motor drive. This method requires power measurement but it does not require the knowledge of motor parameters accurately. When saturation and harmonics effects are considered, the optimal slip depends on load torque and speed. Parviz Famouri et al.[43] presented a microprocessor based adaptive system for operation of an inverter fed induction motor drive to operate at the point of maximum efficiency maintaining any particular load torque speed point. Gyu-Sik-Kim et al.[44], presented a method for power efficiency and good dynamic performance. In this, squared rotor flux is adjusted until the measured power reaches to minimum according to minimum power search algorithm. The controller depends on rotor resistance, hence, this scheme is robust with respect to its variation because identification algorithm is employed. Bimal K. Bose [45] described a fuzzy logic based efficiency optimization control of induction motor drive. In this, two algorithms have been implemented. One is efficiency optimization algorithm that is implemented at steady state and during dynamic response like change in speed or load torque, the optimization algorithm is abandoned because that algorithm reduces the stator flux and constant flux value is applied for good dynamic response. When the response reaches to steady state, then controller is switched back to optimization algorithm after delay of three sampling instants. J.O. Garcia and J.C. Mendes et al.[46] proposed an approach to minimize the total iron and copper losses of variable speed induction drive keeping good dynamic response otherwise in flux weakening related efficiency algorithm, the dynamic response degrades.

Waheeda Bevi M et al. [47] presented a paper for loss minimization of vector controlled induction motor using genetic algorithm (GA). In this, GA is applied to minimize the losses of motor by optimizing the value of magnetizing current. Hence, this algorithm is implemented to optimize the value of direct axis stator current in order to reduce the core losses of the motor. Junzhi Yu et al. [48] designed a novel loss minimization algorithm for induction motor. In this paper, the algorithm is obtained from energy balance equation of the induction drive's port controlled Hamilton model, in which all the parameters are considered and, hence, making it more accurate than conventional loss algorithm. M.C. Di Piazza et al. [49] proposed a benchmark not only to reduce electric loss but also switching losses by Discontinuous PWM and electric loss minimization technique. Srikanthan Sridharan et al. [50, 51] presented overall system loss minimization method to achieve true minimum loss as compared to comprehensive loss model in the induction motor drive. Olorunfemi Ojo et al. [54] reported the steady state optimized operation of induction motor drive above base speed under three field orientation schemes viz. rotor field orientation control, stator flux orientation control and air gap field orientation control.

Conclusions

Various previous IEEE research papers have been read, carefully examined and books for the concerned topic have been read and implementation of one IEEE paper will be done in MATLAB/Simulink environment.

CHAPTER 3

DYNAMIC MODEL OF THE INDUCTION MOTOR

3.1 General

Squirrel cage induction motor is widely used in modern industries because of its cost effectiveness, robust and simple construction as compared to wound rotor induction motor. The weight of squirrel cage rotor is low which results in less windage losses and centrifugal force. While, wound rotor induction motors are used for applications which requires soft starts and adjustable speeds. External resistance can be added to rotor via slip rings which makes it possible for high starting torque, soft starts and low starting current, but it results in losses in resistance. There exist many control techniques like scalar, field oriented control (FOC) or vector control etc. FOC technique provides good dynamic performance of the induction motor drive and in order to implement this, the two dimensional reference frame that is synchronously rotating, rotor and stationary are transformed from three dimensional variables. Therefore, dynamic model of induction motor in direct and quadrature (d – q) reference frame is elaborated. The dynamic model of IM is complex and there are many different forms of the model depending on the choice of reference frame. The voltage and torque equations that describe the dynamic behaviour of induction motor are time-varying. A change of variables can also be used to reduce the complexity of the model by eliminating all time varying inductance. For this it is necessary transform three phase stationary reference variables to a two phase stationary reference frame, Clarke's Transformation is done followed by a transformation to the two phase rotating frame that is called Park's Transformation.

3.2 Transformations for Dynamic Modelling of Induction Motor

The various transformations like Clarke's and Park's Transformation have been done:

- **Clarke's Transformation**

  Two phase stationary reference frame denoted by d^s - q^s are transformed from three phase stationary reference frame variables using this transformation. The symmetrical three phase induction motor with stationary a-b-c axis displaced by 120^0 from each other is shown in figure 3.1. The concerned transformation matrix is given by:

$$\begin{bmatrix} v_{qs}^s \\ v_{ds}^s \\ v_{0s}^s \end{bmatrix} = \frac{2}{3} \begin{bmatrix} \cos\theta & \cos(\theta - 120) & \cos(\theta + 120) \\ \sin\theta & \sin(\theta - 120) & \sin(\theta + 120) \\ 1/2 & 1/2 & 1/2 \end{bmatrix} \begin{bmatrix} v_a \\ v_b \\ v_c \end{bmatrix} \quad 3.1$$

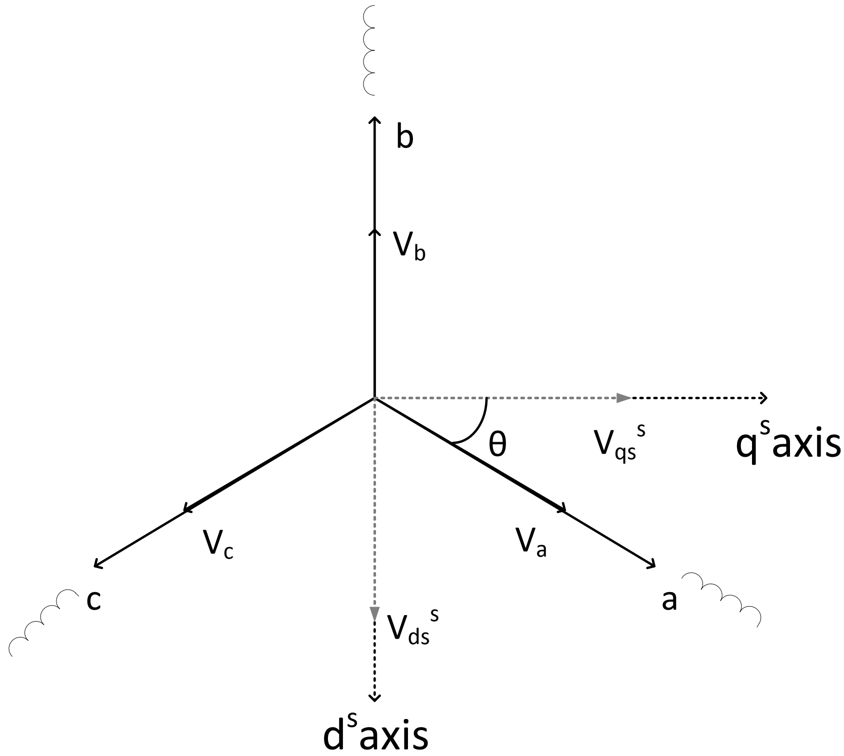

Fig 3.1: Clarke's Transformation

Where v_{0s}^s is added as the zero sequence component which is not present in balanced conditions. When d^s - q^s axes is oriented at an angle θ to a- axis, v_{qs}^s and v_{ds}^s are respectively obtained from phase voltages, v_a, v_b and v_c.

The inverse relation of the above matrix is given by:

$$\begin{bmatrix} v_a \\ v_b \\ v_c \end{bmatrix} = \begin{bmatrix} \cos\theta & \sin\theta & 1 \\ \cos(\theta - 120) & \sin(\theta - 120) & 1 \\ \cos(\theta + 120) & \sin(\theta + 120) & 1 \end{bmatrix} \begin{bmatrix} v_{qs}^s \\ v_{ds}^s \\ v_{0s}^s \end{bmatrix} \quad 3.2$$

If θ = 0, i.e. q^s axis is aligned with a- axis and zero sequence component are ignored then above matrix is given by:

$$\begin{bmatrix} v_a \\ v_b \\ v_c \end{bmatrix} = \begin{bmatrix} 1 & 0 & 1 \\ -1/2 & -\sqrt{3}/2 & 1 \\ -1/2 & \sqrt{3}/2 & 1 \end{bmatrix} \begin{bmatrix} v_{qs}^s \\ v_{ds}^s \\ 0 \end{bmatrix} \qquad 3.3$$

And,

$$\begin{bmatrix} v_{qs}^s \\ v_{ds}^s \\ 0 \end{bmatrix} = \frac{2}{3} \begin{bmatrix} 1 & -1/2 & -1/2 \\ 0 & -\sqrt{3}/2 & \sqrt{3}/2 \\ 1/2 & 1/2 & 1/2 \end{bmatrix} \begin{bmatrix} v_a \\ v_b \\ v_c \end{bmatrix} \qquad 3.4$$

In balanced condition,

$$v_a + v_b + v_c = 0 \qquad 3.5$$

Hence, this conversion is from three phase stationary reference frame ($a - b - c$) to stator reference frame ($d^s - q^s$) in which $d^s and\ q^s$ are orthogonal to each other.

- **Inverse Clarke's Transformation**

  In this transformation two phase orthogonal stationary frame is converted to three phase stationary frame using the following equations:

$$v_a = v_{qs}^s \qquad 3.6$$

$$v_b = \frac{-v_{qs}^s}{2} + \frac{\sqrt{3} * v_{ds}^s}{2} \qquad 3.7$$

$$v_c = \frac{-v_{qs}^s}{2} - \frac{\sqrt{3} * v_{ds}^s}{2} \qquad 3.8$$

  Here, θ = 0 and it can be calculated using figure 3.1.

- **Park's Transformation**

  In this type of transformation, the two phase orthogonal stationary frame ($d - q$) is transformed into two phase rotating frame ($d^e - q^e$). The synchronously rotating axes that rotates at synchronous speed (i.e. ω_e) with respect to the stationary axes at an angle θ_e, as shown in figure 3.2.

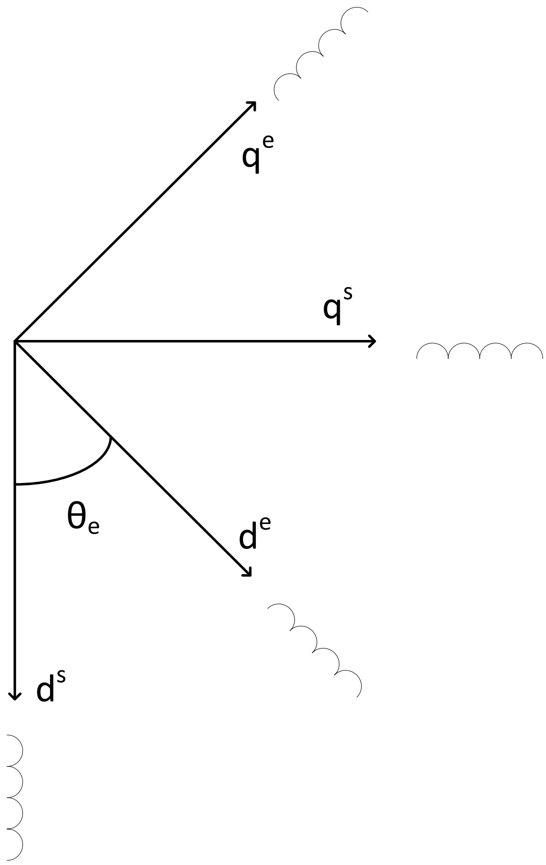

Fig 3.2: Park's Transformation

Here, $\theta_e = \omega_e t$ and v_{qs} and v_{ds} are voltages in synchronously rotating frame. From figure 3.2, the following equations can easily be derived:

$$v_{qs} = v_{qs}^s * \cos\theta_e - v_{ds}^s * \sin\theta_e \quad 3.9$$

$$v_{ds} = v_{qs}^s * \sin\theta_e + v_{ds}^s * \cos\theta_e \quad 3.10$$

And, same can be represented using matrix:

$$\begin{bmatrix} v_{qs} \\ v_{ds} \end{bmatrix} = \begin{bmatrix} \cos\theta_e & -\sin\theta_e \\ \sin\theta_e & \cos\theta_e \end{bmatrix} \begin{bmatrix} v_{qs}^s \\ v_{ds}^s \end{bmatrix} \quad 3.11$$

Also, v_{qs} and v_{ds} can be transformed to v_{qs}^s and v_{ds}^s using Inverse Park's Transformation.

- ## Inverse Park's Transformation

In this type of transformation, the rotating reference frame is transferred to two axis orthogonal stationary frame i.e. $(d^e - q^e)$ frame to $(d^s - q^s)$ frame. Using figure 3.2, this transformation can be done through below equations:

$$v_{qs}^s = v_{qs} * \cos\theta_e + v_{ds} * \sin\theta_e \quad 3.12$$

$$v_{qs}^s = -v_{qs} * \sin\theta_e + v_{ds} * \cos\theta_e \quad 3.13$$

And, same can be shown in matrix form:

$$\begin{bmatrix} v_{qs}^e \\ v_{ds}^e \end{bmatrix} = \begin{bmatrix} \cos\theta_e & \sin\theta_e \\ -\sin\theta_e & \cos\theta_e \end{bmatrix} \begin{bmatrix} v_{qs} \\ v_{ds} \end{bmatrix} \qquad 3.14$$

By using inverse Park's transformation the execution of transformation link between the stationary reference frame and synchronously rotating frame takes place:

$$\begin{bmatrix} v_a \\ v_b \\ v_c \end{bmatrix} = \begin{bmatrix} \cos(\theta_e) & -\sin(\theta_e) \\ \cos(\theta_e - 2\pi/3) & -\sin(\theta_e - 2\pi/3) \\ \cos(\theta_e + 2\pi/3) & -\sin(\theta_e - 2\pi/3) \end{bmatrix} \begin{bmatrix} v_{ds} \\ v_{qs} \end{bmatrix} \qquad 3.15$$

We assume that all the quantities are balanced.

3.3 Dynamic d-q Model of Induction Motor

In the development of the dynamic model of the three phase IM, it is assumed that the motor has three phase symmetrical windings on the stator. The time varying inductances in the voltage equation of the induction motor due to electric circuit in relative motion are eliminated by transferring the stator and rotor variables to a reference frame, which rotates at an angular velocity and remain stationary, viz. stationary reference frame, synchronously rotating frame, rotor reference frame. In this work synchronously rotating reference frame is used, as each variable in the synchronous frame (current, voltage and flux linkage) is stationary and fixed at a constant magnitude in steady state.

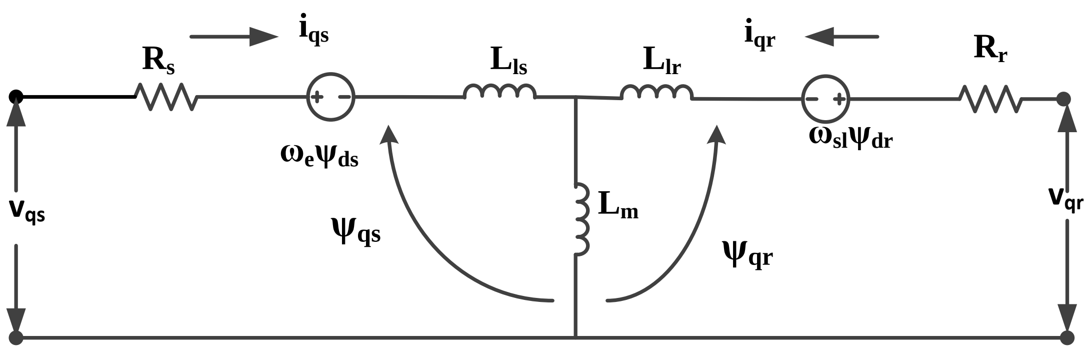

(a)

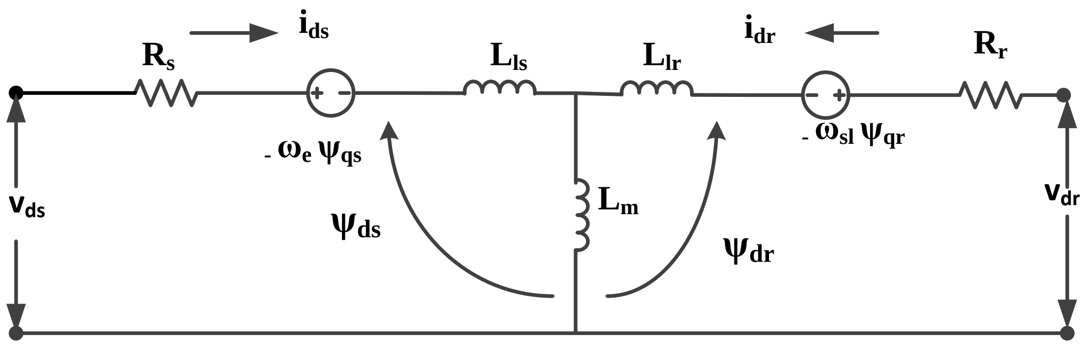

(b)

Fig 3.3(a),(b): Equivalent $q^e - d^e$ circuit model of Induction Motor(IM)

Here, all the rotor and stator variables are transformed in the synchronously rotating reference frame. The equations of voltages of stator in that frame are given by:

$$v_{qs} = i_{qs}R_s + \frac{d}{dt}\Psi_{qs} + \omega_e\Psi_{ds} \quad 3.16$$

$$v_{qs} = i_{ds}R_s + \frac{d}{dt}\Psi_{ds} - \omega_e\Psi_{qs} \quad 3.17$$

Where,

R_s - Stator resistance

Ψ_{ds}, Ψ_{qs} - $d^e - q^e$ axes stator flux linkage

i_{ds}, i_{qs} - $d^e - q^e$ axes stator current

Also, equations of voltages of rotor in synchronous frame and rotor is running in the magnetic field direction at an angular speed, ω_r:

$$v_{qr} = i_{qr}R_r + \frac{d}{dt}\Psi_{qr} + (\omega_e - \omega_r)\Psi_{dr} = 0 \quad 3.18$$

$$v_{qr} = i_{dr}R_r + \frac{d}{dt}\Psi_{dr} + (\omega_e - \omega_r)\Psi_{qr} = 0 \quad 3.19$$

Where,

R_r – Resistance of rotor

Ψ_{dr}, Ψ_{qr} - $d^e - q^e$ axis flux linkage on rotor

i_{dr}, i_{qr} - $d^e - q^e$ axis current on rotor side

The flux linkages equations can also be written in terms of inductance and current:

$$\Psi_{qs} = i_{qs}L_{ls} + L_m\left(i_{qs} + i_{qr}\right) = L_s i_{qs} + L_m i_{qr} \quad 3.20$$

$\Psi_{qr} = i_{qr}L_{lr} + L_m(i_{qs} + i_{qr}) = L_r i_{qr} + L_m i_{qs}$ 3.21

$\Psi_{qm} = L_m(i_{qs} + i_{qr})$ 3.22

$\Psi_{ds} = i_{ds}L_{ls} + L_m(i_{ds} + i_{dr}) = L_s i_{ds} + L_m i_{dr}$ 3.23

$\Psi_{dr} = i_{dr}L_{lr} + L_m(i_{ds} + i_{dr}) = L_r i_{dr} + L_m i_{ds}$ 3.24

$\Psi_{dm} = L_m(i_{ds} + i_{dr})$ 3.25

From equations

$$\begin{bmatrix} v_{qs} \\ v_{ds} \\ v_{qr} \\ v_{dr} \end{bmatrix} = \begin{bmatrix} R_s + sL_s & \omega_e L_s & sL_m & \omega_e L_m \\ -\omega_e L_s & R_s + sL_s & -\omega_e L_m & sL_m \\ sL_m & (\omega_e - \omega_r)L_m & R_r + sL_r & (\omega_e - \omega_r)L_r \\ -(\omega_e - \omega_r)L_m & sL_m & -(\omega_e - \omega_r)L_r & R_r + sL_r \end{bmatrix} \begin{bmatrix} i_{qs} \\ i_{ds} \\ i_{qr} \\ i_{dr} \end{bmatrix} \quad 3.26$$

Where,

$L_{s,}L_r$ – Self inductance of stator and rotor

L_m – Mutual inductance

$L_{ls,}L_{lr}$ – Leakage inductance of stator and rotor

Ψ_{dm}, Ψ_{qm} - $d^e - q^e$ axis flux linkage magnetising component

Now, ω_r is a variable and it's relation with electromagnetic torque, T_e is given by:

$T_e - T_L = J\frac{d\omega_m}{dt}$ 3.27

This equation can also be written in electrical form which is as follow:

$T_e - T_L = \frac{2}{P}J\frac{d\omega_r}{dt}$ 3.28

Where,

ω_m – Motor speed in mechanical rad/s

J – Motor Inertia

P – Number of poles of motor

T_L – Load torque

The electromagnetic torque, T_e which is developed due to the interaction of air gap flux Ψ_m and rotor MMF that is dependent on the current flowing in rotor, I_r is expressed in vector form:

$$T_e = \frac{3}{2}\frac{P}{2}\bar{\Psi}_m \times \bar{I}_r \quad 3.29$$

The above vector variables can also be revolved in $d^e - q^e$(synchronous frame) components, according to figure 3.4:

$$T_e = \frac{3}{2}\frac{P}{2}\left(\Psi_{dm} i_{qr} - \Psi_{qm} i_{dr}\right) \quad 3.30$$

Similarly, other torque equations can also easily be derived:

$$T_e = \frac{3}{2}\frac{P}{2}\left(\Psi_{dm} i_{qs} - \Psi_{qm} i_{ds}\right) \quad 3.31$$

$$T_e = \frac{3}{2}\frac{P}{2}\left(\Psi_{ds} i_{qs} - \Psi_{qs} i_{ds}\right) \quad 3.32$$

$$T_e = \frac{3}{2}\frac{P}{2}L_m\left(i_{qs} i_{dr} - i_{ds} i_{qr}\right) \quad 3.33$$

$$T_e = \frac{3}{2}\frac{P}{2}\left(\Psi_{dr} i_{qr} - \Psi_{qr} i_{dr}\right) \quad 3.34$$

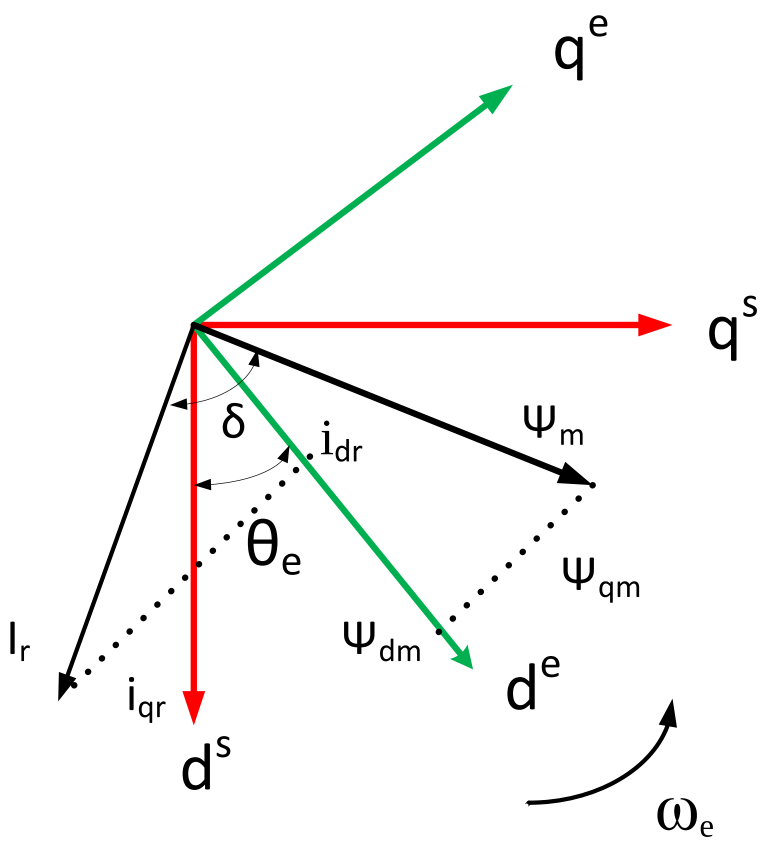

Fig 3.4: $d^e - q^e$ Frame

3.4 Conclusion

In this chapter, the various transformations that are used to study dynamic model of the induction motor has been discussed. Using synchronous frame the inductances that are time varying appeared in equation of voltages etc has been eliminated. Further, different equations of electromagnetic torque have also been derived. Now, this dynamic model of motor will help in implementing the various methods of vector control technique that will be discussed in next chapter.

CHAPTER 4

TECHNIQUES TO CONTROL INDUCTION MOTOR

4.1 General

Induction motor drives are widely used in industries for various applications because of their high torque to weight ratio as compared to DC motor, robust structure, sustainable to operate in hazardous place. However, due to their complex and nonlinear structure control of induction motor is a challenging task. The main reason behind this complexity is requirement of variable frequency, harmonically optimum converter power supplies, Complex dynamic of ac machines, and variation in machine parameters. Also, power electronics devices has also become sophisticated in few decades that is attracting various industries to use this in drives. In this chapter the various research on modelling of induction motor and its control strategies are discussed. Usually, for variable speed applications the induction motors are fed through inverters and this type of drive is also called AC Motor Drive. Since, the dynamic model of the induction motor has been discussed in previous chapter. So, in this chapter the various control techniques for adjustable speed operation of induction motor, which is fed through induction motor is discussed.

Voltage Source Inverter (VSI) fed induction motor is generally used for variable voltage variable frequency (VVVF) drive. Pulse Width Modulation (PWM) control technique is used to control the speed, position and torque control. Generally, PWM signals are low power signals hence, it cannot be used directly in the gate terminal of IGBTs and MOSFETs. Therefore, a gate driver circuit is used to isolate high power and low power circuit. It provides constant voltage gate pulse of variable width depending on the controller operation. Hence, these signals will help to achieve speed and torque control options.

Artificial Intelligence (AI) has also gained importance with time. As, these techniques are used where the knowledge of mathematical model of system is not known. Hence, this technique will try to give optimize results that are less accurate as compared with a mathematical model. Various terms have been used in this area like fuzzy logic (FL), artificial neural network (ANN) and genetic algorithm (GA) and all these have been classified into soft computing or approximate computing. In this research work, fuzzy inference system (FIS) has been implemented in the MATLAB simulation.

4.2 Methods to Control Induction Motor

This includes various techniques for controlling the speed of induction motor like Scalar Control, Vector or Field Oriented Control that consists of direct or feedback vector control and indirect vector control, all these methods will be briefly described in subsequent sections.

4.2.1 Scalar Control

Scalar control of induction motor is mainly based on steady state model of motor. In scalar control, only magnitudes of input variables like frequency and voltage are controlled. Flux control is achieved through variation of voltage and torque control is achieved through variation in frequency and slip. However, flux and torque being functions of frequency and voltage respectively, there is an inherent coupling effects in the flux and torque producing components. Due to coupling effects between torque and flux, the dynamic response of machine is reduced which will tend the system at the verge of instability. There are two types of scalar control techniques. First is open loop V/f speed control and second is close loop V/f control.

Figure 4.1 shows the open loop V/f control in which ω_e^* is the controlled input variable and speed will change according to its variation. A function generator is placed between V_o and ω_e^* to maintain V/f ratio constant. Hence, with increase or decrease in frequency, the voltage will also vary accordingly. Then, V_o and ω_e^* will be used to generate pulses from PWM controller and these pulses are then fed to gate terminals of switching devices.

In closed loop V/f control, the problem of the variation in the air gap flux because of fluctuation in the line voltage and drop-in impedance that has been observed in open loop V/f control has been overcome. Here, the error is generated in the speed feedback and ω_{sl}^* is generated through PI controller and speed limiter. This slip speed is added to ω_r to produce ω_e^*. Further process is similar to open loop V/f control as shown in the figure 4.2.

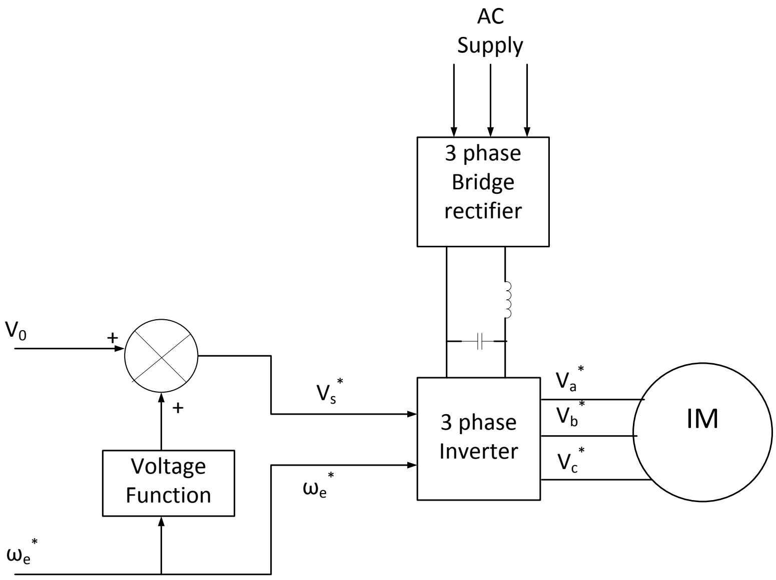

Figure 4.1: Open loop V/f control of induction motor

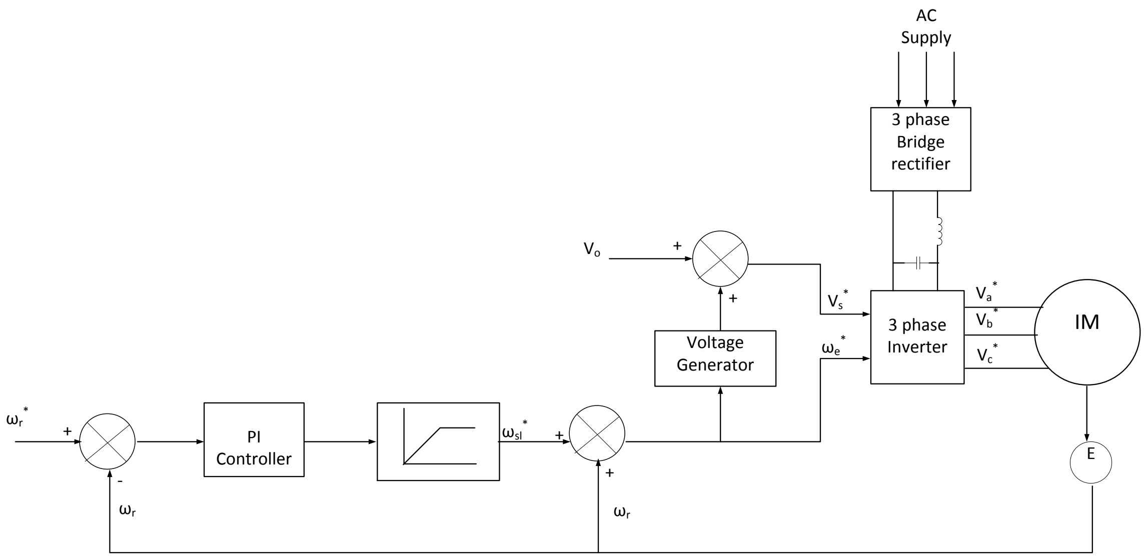

Figure 4.2: Close loop V/f control of induction motor

4.2.2 Vector Control

In recent years field oriented control (FOC) or vector control is widely used in industries because of fast response similar to DC motor, as change in one variable will not affect the other variable in dynamic process. The stator current splits in two orthogonal components, one is the flux component or magnetizing current and other one is the torque component both the components can vary independently, Induction machine will be treated as similar to separately excited DC machine.

4.2.2.1 DC Machine Analogy

A vector controlled induction machine operates like a separately excited DC machine as shown in figure 4.3:

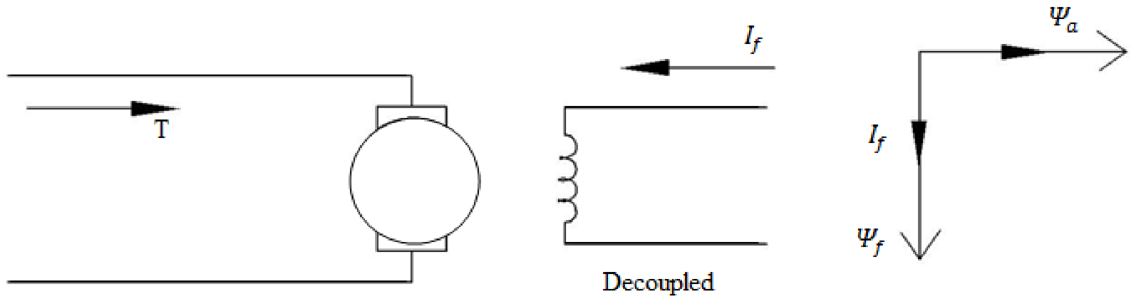

Figure 4.3: Seprately excited DC Motor

The electromagnetic of DC machine is given by:

$T_e = K_t \Psi_f \Psi_a$ or, 4.1

$T_e = K_t I_f I_a$ 4.2

Where,

Ψ_f, Ψ_a – Field and armature flux

I_f, I_a – Field and armature current

In construction of dc motor the field flux (Ψ_f) developed or generated by the field current (I_f) is at 90 degrees out of phase to armature flux (Ψ_a), which is developed by the armature current (I_a). These space vectors are stationary in space, but they are decoupled and orthogonal in nature. When armature current is changed for controlling the torque, there will be no effect on field flux hence there will be fast transient response. Similarly, when the field flux (Ψ_f) is changed, there will be no effect on armature flux (Ψ_a). Induction motor has a disadvantage that it cannot give a fast response due to the inherent coupling problem. Induction motor can give a performance like an DC motor, if machine will be in $d^e - q^e$synchronously rotating reference frame. As in steady state condition, sinusoidal variables will appear similar to dc quantity.

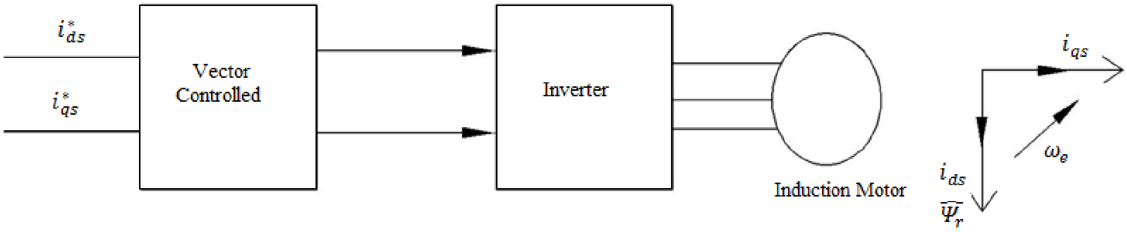

Figure 4.4 : Vector-Controlled Induction Motor

In figure 4.4, the induction motor is shown with vector control with two input control current input (i_{ds}^*, i_{qs}^*) and inverter connected to induction motor from the front side. These are the direct and the quadratue axis stator current component in a synchronously rotating reference frame. In vector control, i_{ds} is similar to current flowing in the field (I_f) and I_{qs} is same as armature current (I_a) of a dc motor. Now, the torque is given by:

$T_e = K_t \Psi_r' I_{qs}$ or, 4.3

$T_e = K_t' I_{ds} I_{qs}$ 4.4

Where,

Ψ'_r = peak value of sinusoidal space vector

Induction machines gives a performance similar to dc machine only when I_{ds} is in phase in the direction of direct axis Ψ'_r and current in quadrature axis I_{qs} is at 90 degrees to it as shown in figure 4.4. This concludes that when current I_{qs} is controlled, it only affects the actual current I_{qs} and there will be no effect on flux, and when current I_{ds} is controlled it only affects the flux component but there will be no effect on current I_{qs}. In field oriented control or vector control drive current is mandatory in all operating conditions. In comparison of DC machine, AC machine space vector rotates synchronously at frequency ω_e.

As compared to Vector control, Scalar control is very simple and easy to implement, torque and flux are basically dependent on current or voltage and frequency but due to coupling effects, it gives very sluggish response, and because of higher order harmonics system will move towards instability. We take an example if slip will increase the torque will increase, and with that the flux will decrease. Variation of flux will give sluggish response. These problems can be rectified through field oriented control (vector control). Vector control was invented in 1970s, and it was prove that an induction motor can be driven like a DC motor, it gives rejuvenation in the performance of AC drives. Decoupling and orthogonal control is known for vector control, as a performance is similar to a dc machine. Vector control can also be used for permanent magnet synchronous motor and various ratings of induction motors.is not only used for induction motor but it is also applicable for synchronous machine drives. The use of DSP and microcomputer is mandatory for sensor less motors because of its high complexity as feedback signals are used for vector control.

4.2.2.2 Vector Control Principle-

The machine model vector controlled principle can be explained by various reference frames and here synchronous frame is used for explanation. We assume unity current gain for inverter and hence not shown in the figure and i_{abc} are controlled by $i_{abc}^*$from the controller. The conversion or transformations like $d^e - q^e$ to $d^s - q^s$ and $d^s - q^s$ to $a - b - c$ of the inverse transformation model is given on the left side of figure. Similarly, i_{abc} to I_{ds}^s - I_{qs}^s transformation on right side is done by using Clarke's transformation. Similarly, other transformations are also used before fed into the machine model.

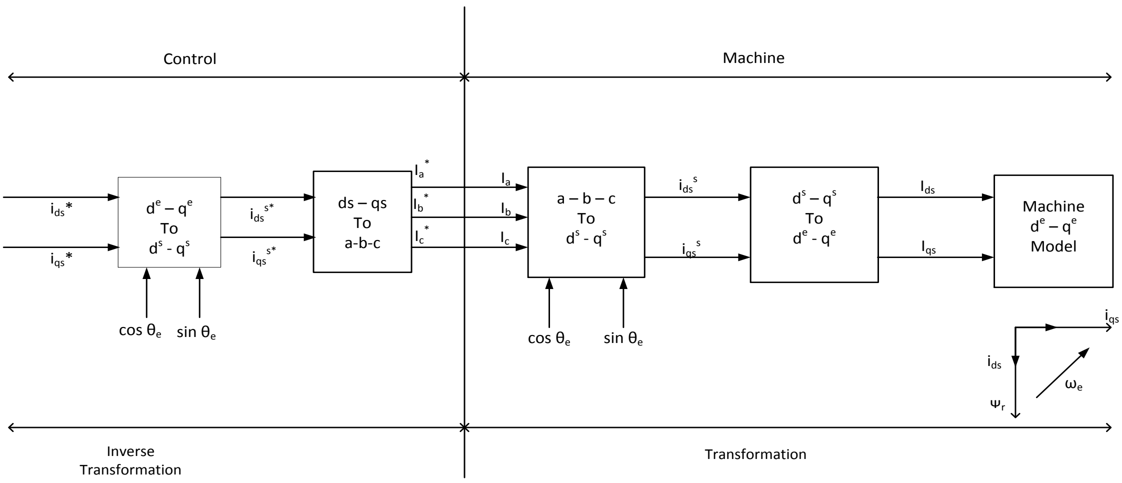

Figure 4.5- Vector Control Principle in $d^e - q^e$ model

The transformation will first transform the synchronous frame to stationary with the help of unit vectors $\sin\theta_e$ and $\cos\theta_e$ and generates I_{ds}^* and I_{qs}^* currents which is then converted to $a - b - c$ controlling variables which is then fed to the machine. Then, again same transformations are again done in reverse order which is then fed motor for vector control.

4.2.2.3 Types of Vector Control

The types of vector control are direct and indirect vector control that is discussed:

1. Direct or Feedback Vector Control

The controls parameters are i_{ds}^{*} and i_{qs}^{*} that are generated in feedback path in synchronously rotating reference frame is the beauty of this vector control. It is first transformed to stationary reference frame using vector rotation. Field flux signals Ψ_{dr}^{s} and Ψ_{qr}^{s} that are evaluated using voltages and currents of the induction motor. The output torque component so obtained by the current i_{qs}^{*} is generated from the speed control loop through a torque limiter. The flux component of the current i_{ds}^{*} is generated from flux loop, which are converted to stationary frame using θ_e and then to abc variables. For the implementation of this scheme magnitude of rotor flux and its position is essential. The $\widehat{\Psi_r}$ flux is aligned or in phase in the direction of current i_{ds} and also i_{qs} quadrature current is perpendicular to flux. In figure 4.7, vectors of rotor flux in stationary reference frame Ψ_{dr}^{s} and Ψ_{qr}^{s} are shown. The stationary frame d^s-q^s and the frame d^e-q^e which is rotating with synchronous speed ω_e, the phase angle between the stationary frame and synchronous frame is θ_e and the same is equivalent to ω_et.

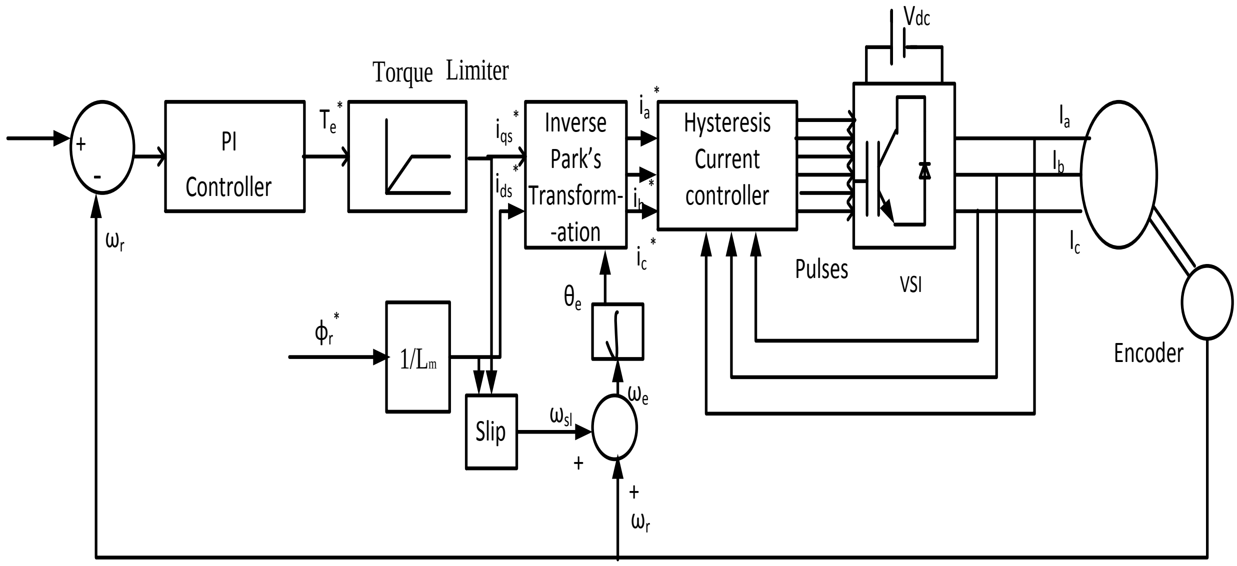

Figure 4.6: Schematic diagram of direct vector control

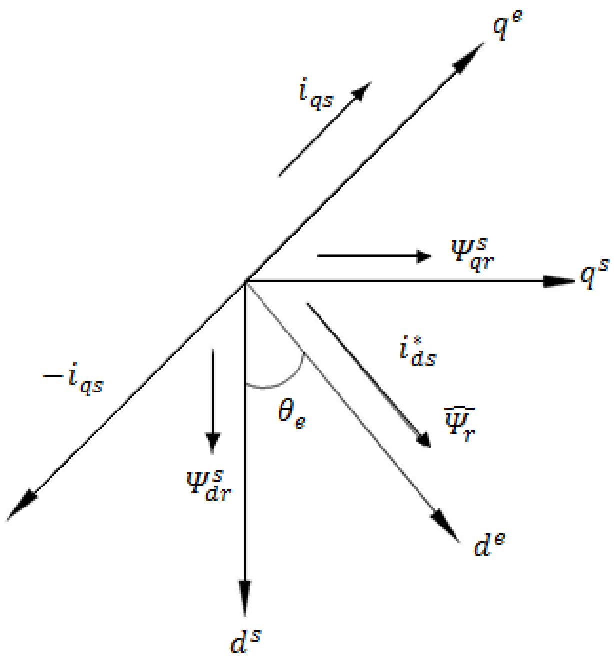

Figure 4.7: Rotor flux orientation in $d^e - q^e$ and $d^s - q^s$ phasors

The following equations can be obtained using figure 4.7:

$$\Psi^s_{dr} = \widehat{\Psi}_r cos\ \theta_e \qquad 4.5$$

$$\Psi^s_{qr} = \widehat{\Psi}_r sin\ \theta_e \qquad 4.6$$

$$cos\ \theta_e = \frac{\Psi^s_{dr}}{\widehat{\Psi}_r} \qquad 4.7$$

$$sin\ \theta_e = \frac{\Psi^s_{qr}}{\widehat{\Psi}_r} \qquad 4.8$$

$$\widehat{\Psi}_r = \sqrt{{\Psi^s_{dr}}^2 + {\Psi^s_{qr}}^2} \qquad 4.9$$

Form figure 4.8, sin θ_e and $cos\ \theta_e$ are unit vector signals, when used for vector rotation. It gives a ride of current i_{ds} on the d^e (direction of $\widehat{\Psi}_r$) and current i_{qs} on the q^e- axis.

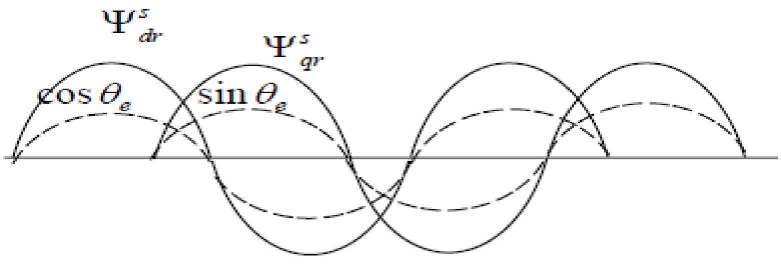

Figure 4.8: Unit Vector Position in correct phase condition

VECTOR CONTROL FEATURES

1. The phase and synchronous frequency are controlled with unit vector. Therefore, the machine is self controlled as the angular synchronous frequency (ω_e) cannot be controlled directly.
2. If the set point of torque is beyond the breakdown torque T_{em} then there will be no problem of instability as the current will remain in safe values that is automatically be performed by vector control.
3. There exist two orthogonal trajectories as change in one will not affect the other hence, results in good dynamic response. Change in i_{qs} will affect torque only not flux.
4. Ideal vector control is not possible because there exist some delays in components. Hence, signal processing and variation in parameters will have some effects.
5. Using vector control, the motor can be operated in all four quadrants of torque and speed characteristics without using extra components like for reversing the speed, phase reversal is required.
6. Variation of temperature will change the parameters like inductance and resistance that can reduce the system accuracy. But, these can now be compensated using MRAS techniques. Also, at high voltages these effects can be reduced.

2. Indirect Vector Control

The difference between the direct vector control and indirect vector control is that indirect vector control is somewhat easy to implement and unit vectors will be produced in feed forward control. Otherwise, it is very much similar to direct vector control. Since this vector control is easy to implement hence it is used in industrial application. The concerned principle of indirect vector control can be demonstrated using phasor diagram that is shown in the figure 4.9:

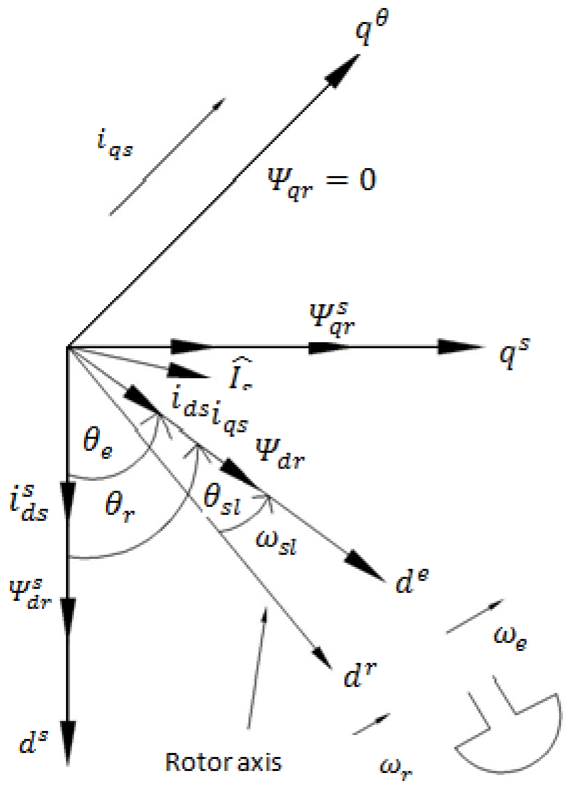

Figure 4.9:Indirect Vector Control phasor diagram

The rotating axis ($d^r - q^r$) is fixed on the rotor terminals while the stationary axis ($d^e - q^e$) is fixed on the stator frame, the rotating axis is rotating at a speed ω_r and is shown in Figure 4.9. The rotating axis ($d^r - q^r$) lags the synchronously rotating axes ($d^e - q^e$) by slip angle (θ_{sl}) that is the integration of slip frequency (ω_{sl}) with respect to time. Therefore, the equation can be formed:

$$\omega_e = \omega_r + \omega_{sl} \tag{4.10}$$

Also the below equation can also be formed:

$$\theta_e = \int \omega_e dt = \int \omega_r + \omega_{sl} dt = \theta_r + \theta_{sl} \tag{4.11}$$

The flux vector can also be estimated from the machine model using the voltage model. The fluxes are evaluated using $d^{s}-q^{s}$ stationary frame of reference as voltage and current can be observed. The following equations of flux are:

$$\Psi_{ds}^{s} = \int (v_{ds}^{s} - R_s i_{ds}^{s}) dt \tag{4.12}$$

$$\Psi_{qs}^{s} = \int (v_{qs}^{s} - R_s i_{qs}^{s}) dt \tag{4.13}$$

$$\Psi_{r}^{s2} = \Psi_{dr}^{s\ 2} + \Psi_{dr}^{s\ 2} \tag{4.14}$$

$$\Psi_{dm}^{s} = \Psi_{ds}^{s} - L_{ls} i_{ds}^{s} = L_m(i_{ds}^{s} + i_{dr}^{s}) \qquad 4.15$$

$$\Psi_{qm}^{s} = \Psi_{qs}^{s} - L_{ls} i_{qs}^{s} = L_m(i_{qs}^{s} + i_{qr}^{s}) \qquad 4.16$$

$$\Psi_{dr}^{s} = L_m\, i_{ds}^{s} + L_r i_{dr}^{s} \qquad 4.17$$

$$\Psi_{qr}^{s} = L_m\, i_{qs}^{s} + L_r i_{qr}^{s} \qquad 4.18$$

i_{dr}^{s} and i_{qr}^{s} can be eliminated from the equations above 4.17 and 4.18 and using that in equations 4.15 and 4.16 yields:

$$\Psi_{dr}^{s} = \frac{L_r}{L_m}\Psi_{dm}^{s} - L_{lr} i_{ds}^{s} \qquad 4.19$$

$$\Psi_{qr}^{s} = \frac{L_r}{L_m}\Psi_{qm}^{s} - L_{lr} i_{qs}^{s} \qquad 4.20$$

Now, derivation of concerned control technique equations is a major issue. Therefore, the equations will be:

$$\frac{d\Psi_{dr}}{dt} + R_r i_{dr} - (\omega_e - \omega_r)\Psi_{qr} = 0 \qquad 4.21$$

$$\frac{d\Psi_{qr}}{dt} + R_r i_{qr} + (\omega_e - \omega_r)\Psi_{dr} = 0 \qquad 4.22$$

The equations of flux of rotor are as follows:

$$\Psi_{dr} = L_r\, i_{dr} + L_m\, i_{ds} \qquad 4.23$$

$$\Psi_{qr} = L_r\, i_{qr} + L_m\, i_{qs} \qquad 4.24$$

Currents can be computed using above equations:

$$i_{dr} = \frac{1}{L_r}\Psi_{dr} - \frac{L_m}{L_r} i_{ds} \qquad 4.25$$

$$i_{qr} = \frac{1}{L_r}\Psi_{qr} - \frac{L_m}{L_r} i_{qs} \qquad 4.26$$

To eliminate the rotor currents from the equations 4.21 and 4.22 and using the values from equation 4.25 and 2.26 are as follows:

$$\frac{d\Psi_{dr}}{dt} + \frac{R_r}{L_r}\Psi_{dr} - \frac{L_m}{L_r} R_r i_{ds} - \omega_{sl}\Psi_{qr} = 0 \qquad 4.27$$

$$\frac{d\Psi_{qr}}{dt}+\frac{R_r}{L_r}\Psi_{qr}-\frac{L_m}{L_r}R_r i_{qs}-\omega_{sl}\Psi_{dr}\ =0 \qquad 4.28$$

Where $\omega_{sl}=\omega_e-\omega_r$

The desired conditions for decoupling control is:

$\Psi_{qr}=0$,And

$$\frac{d\Psi_{qr}}{dt}=0$$

When the above conditions is substituted, it yields:

$$\frac{L_r}{R_r}\frac{d\widehat{\Psi}_r}{dt}+\widehat{\Psi_r}=L_m i_{ds} \qquad 4.29$$

$$\omega_{sl}=\frac{L_m R_r}{L_r\widehat{\Psi}_r}i_{qs} \qquad 4.30$$

$$\widehat{\Psi_r}=\Psi_{dr}$$

$$\widehat{\Psi_r}=L_m i_{ds} \qquad 4.31$$

The above condition yields that in steady state, rotor flux $\widehat{\Psi_r}$ is directly proportional to i_{ds} current. The block diagram of indirect vector control of induction motor is shown in figure 4.10

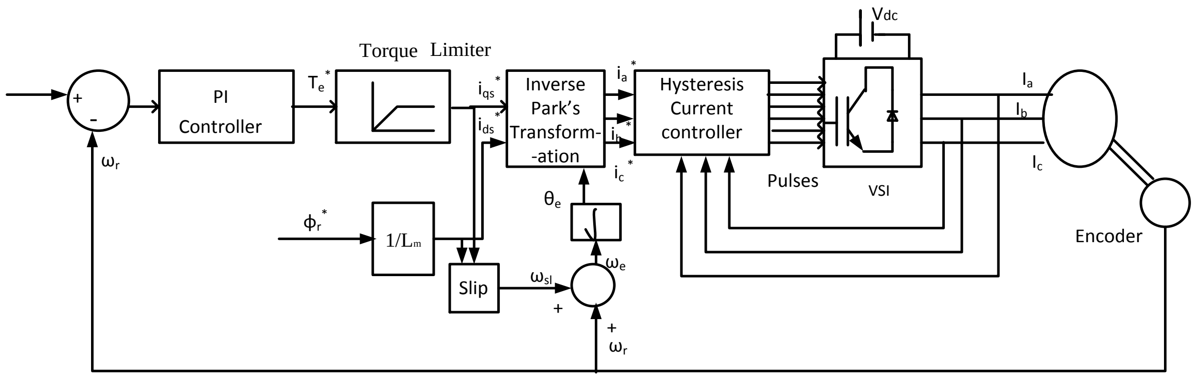

Figure 4.10: Indirect vector control of Induction motor

4.2.3 Hysteresis-Band Current Controller

It is an instantaneous negative feedback current control method in which the actual current chases the reference current within the hysteresis band. This controller generates the reference current wave of desired frequency and magnitude, and it is compared with the actual wave. In this research work, three phase voltage source inverter is used. Hence, three hysteresis band of width ‘δ’ are defined around their respective phase currents. As these three currents are dependent from each other, hence, the system is transformed to (α,β) co-ordinate axis which is similar to stationary reference frame.

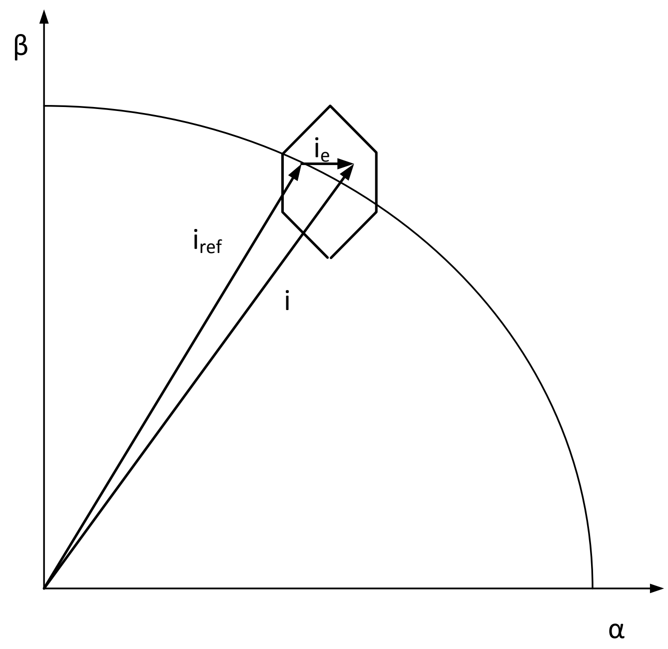

(a)

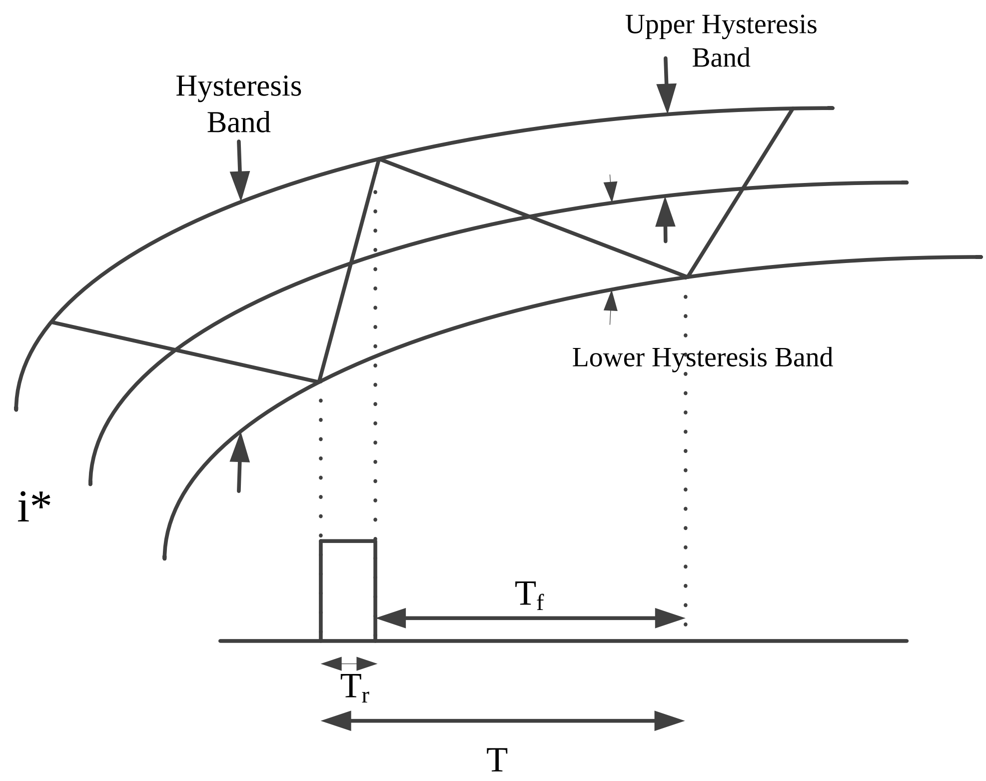

(b)

Figure 4.11(a),(b): Hysteresis current controller

When three hysteresis bands are transformed into this co-ordinate system, this will result in hysteresis hexagonal area. In steady state, the reference current i_{ref} rotates on circle round the origin as shown in figure 4.11. The realistic value of current i has to be kept within the area of hexagon. Hence, each time when tip of i touches the border of the surface that is heading out of the hexagon, the inverter has to be switched accordingly in order to keep the current in the area of hexagon.

4.2.4 Space Vector Pulse Width Modulation (SVPWM)

Space Vector Pulse Width Modulation (SVPWM) is an algorithm which translates phase voltage references (i.e. phase to neutral) coming from controller into duty cycles that can be applied to PWM peripherals like IGBT bridge or MOSFET bridge.

Space Vector Pulse Width Modulation for 3-phase VSI

The topology of a three-leg voltage source inverter is shown in Fig. 4.12. Because of the constraint that the input lines must never be shorted and the output current must always be continuous a voltage source inverter can assume only eight distinct topologies. These topologies are shown on Fig. 4.13. Six out of these eight topologies produce a nonzero output voltage and are known as non-zero switching states and the remaining two topologies produce zero output voltage and are known as zero switching states.

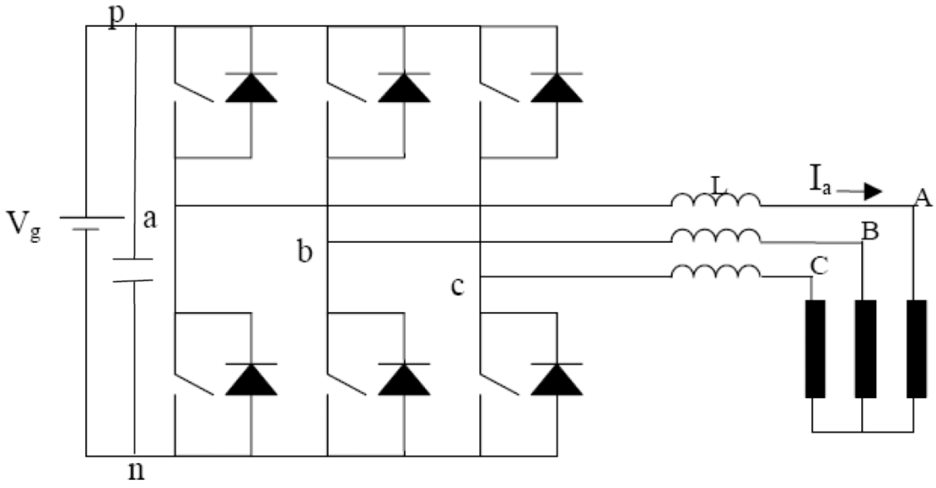

Figure 4.12: Topology for three phase Voltage source inverter

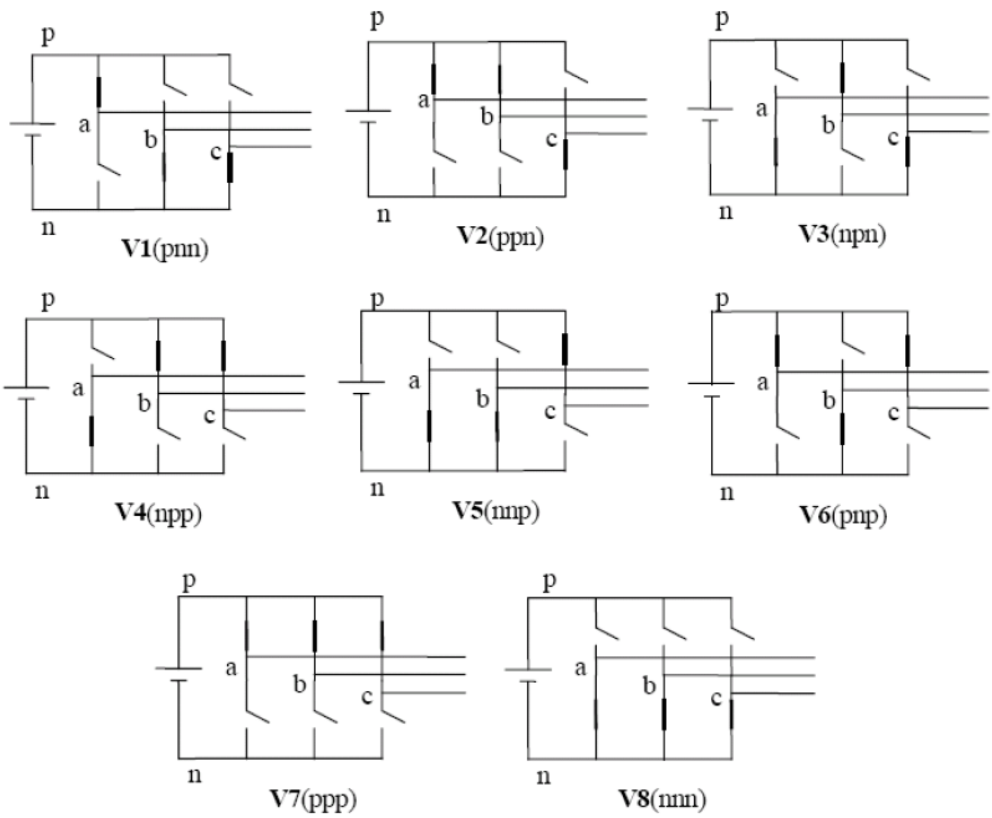

Figure 4.13: Eight Switching state topology of Voltage Source Inverter

Space vector modulation (SVM) for three-leg VSI is based on the representation of the three phase quantities as vectors in a two-dimensional (α,β) plane. This is illustrated here for the sake of completeness. Considering topology 1 of Fig. 4.14, which is repeated in Fig. 11(a) we see that the line voltages V_{ab}, V_{bc}, and V_{ca} are given by:

$$V_{ab} = V_g \tag{4.32}$$

$$V_{bc} = 0 \tag{4.33}$$

$$V_{ca} = -V_g \tag{4.34}$$

This can be represented in the α β, plane as shown in Fig. 4.15, where voltages V_{ab}, V_{bc}, and V_{ca} are three line voltage vectors displaced 120 degree in space. The effective voltage vector generated by this topology is represented as V_1 (pnn) in Fig. 4.15. Here the notation 'pnn' refers to the three legs/phases a,b,c being either connected to the positive dc rail (p) or to the negative dc rail (n). Thus 'pnn' corresponds to phase a. being connected to the positive dc rail and phases b and c being connected to the negative dc rail.

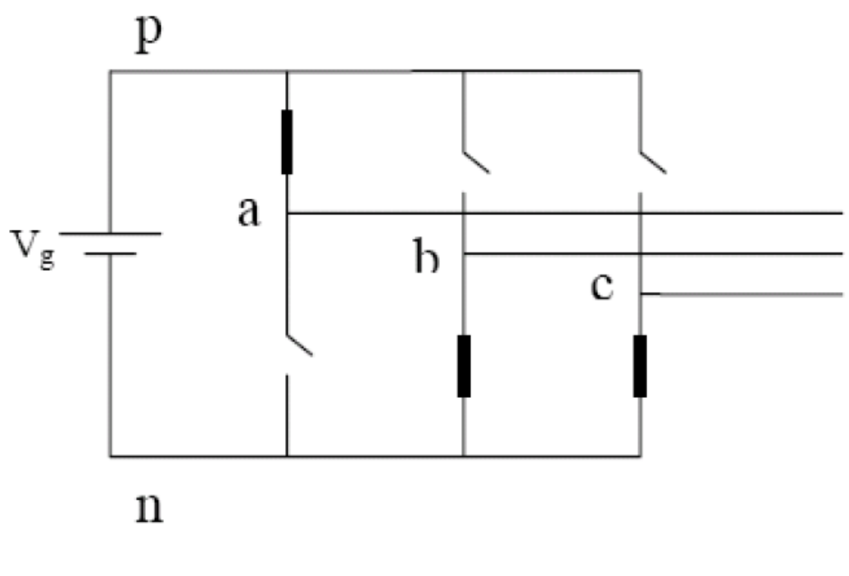

Figure 4.14 : I-VI (pnn) Voltage Source Inverter

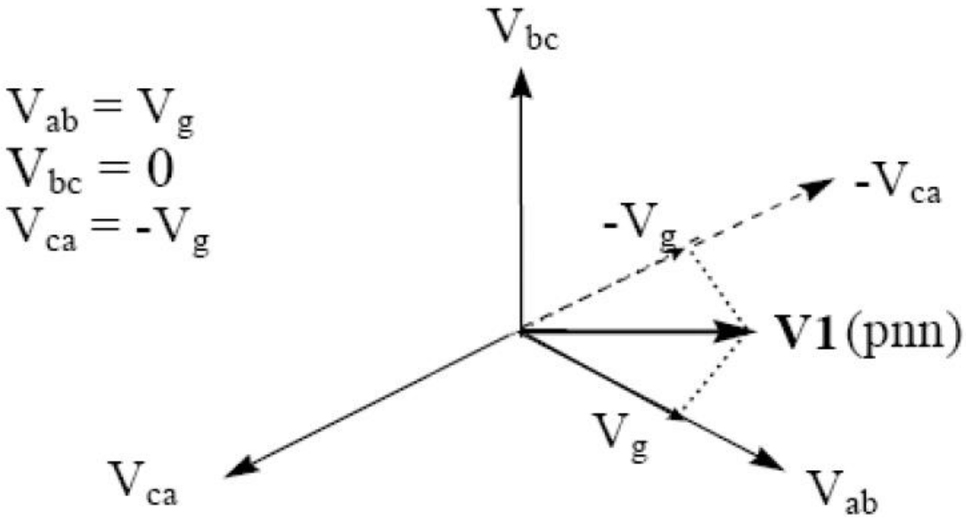

Figure 4.15: Representation of Topology I in α,β plane

Proceeding on similar lines the six non-zero voltage vectors (V_1 - V_6) can be shown to assume the positions shown in Fig.4.16. The tips of these vectors form a regular hexagon (dotted line in Fig. 4.16). We define the area enclosed by two adjacent vectors, within the hexagon, as a sector. Thus there are six sectors numbered 1 - 6 in Fig. 4.16.

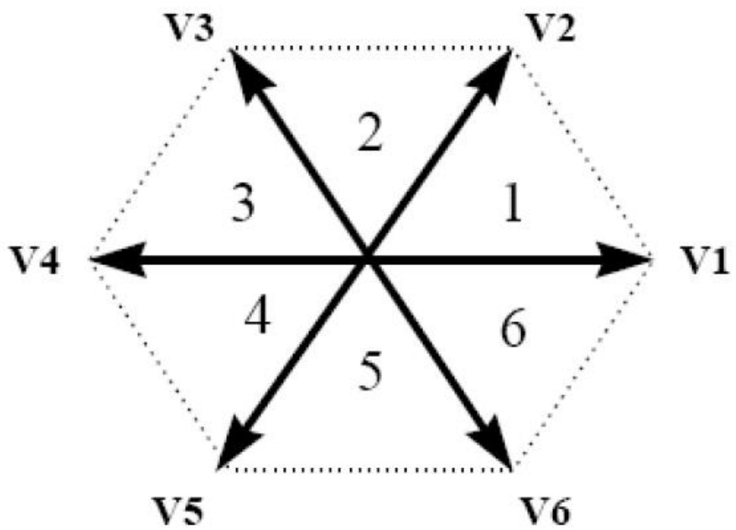

Figure 4.16 : Non Zero Voltage Vectors in α-β plane

Space Vector Modulation

The desired three phase voltages at the output of the inverter could be represented by an equivalent vector V rotating in the counter clock wise direction as shown in Fig. 4.17. The magnitude of this vector is related to the magnitude of the output voltage (Fig. 4.17) and the time this vector takes to complete one revolution is the same as the fundamental time period of the output voltage.

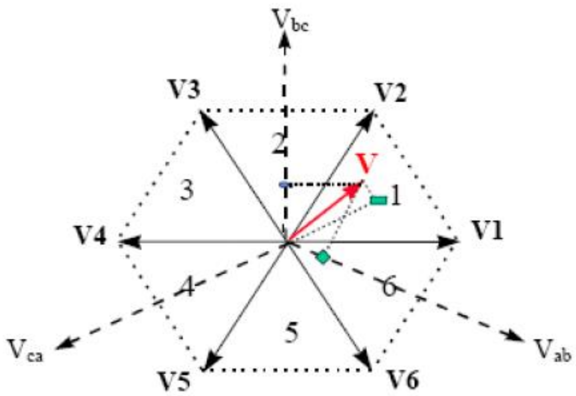

Figure 4.17: Output voltage vector in α,β plane

Let us consider the situation when the desired line-to-line output voltage vector V is in sector 1 as shown in Fig. 4.18. This vector could be synthesized by the pulse-width modulation (PWM) of the two adjacent SSV's V_1 (pnn) and V_2 (ppn), the duty cycle of each being d_1 and d_2, respectively, and the zero vector (V_7(nnn) / V_8(ppp)) of duty cycle d_0:

$$d_1V_1 + d_2V_2 = V = mV_g e^{j\theta} \qquad 4.35$$

$$d_1 + d_2 + d_0 = 1 \qquad 4.36$$

Where, 0< m <0.866, is the modulation index. This would correspond to a maximum line-to line voltage of 1.0Vg, which is 15% more than conventional sinusoidal PWM as shown.

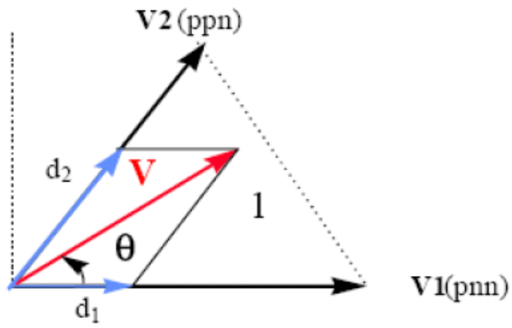

Figure 4.18: Synthesis of output voltage vector in Sector I

All SVM schemes and most of the other PWM algorithms use Eqns. (14) and (15) for the output voltage synthesis. The modulation algorithms that use non-adjacent SSV.s have been shown to produce higher THD and/or switching losses and are not analyzed here, although some of them, e.g. hysteresis, can be very simple to implement and can provide faster transient response. The duty cycles d1, d2, and d0, are uniquely determined from Fig. 2.7, and Eqns. (14) and (15) , the only difference between PWM schemes that use adjacent vectors is the choice of the zero vector(s) and the sequence in which the vectors are applied within the switching cycle.

The degrees of freedom we have in the choice of a given modulation algorithm is:

1) The choice of the zero vector; whether we would like to use V7(ppp) or V8(nnn) or both,

2) Sequencing of the vectors

3) Splitting of the duty cycles of the vectors without introducing additional commutations.

Implementing SVPWM

The SVPWM can be implemented by using wither sector selection algorithm or by using a carrier based space vector algorithm.

The types of SVPWM implementations are:-

a) Sector selection based space vector modulation

b) Reduced switching Space vector modulation

c) Carrier based space vector modulation

d) Reduced switching carrier based space vector modulation.

1. Sector selection based SVPWM:

The figure below above provides an idea of the sector selection based space vector modulation. We have implanted the same using the Simulink blocks and s-functions algorithms wherever needed.

2. Reduced switching SVPWM:

The switching of the IGBTs can be reduced by 33% by choosing to use one of the zero vectors during each sector.

4.3.3 Carrier Based SVPWM:

Carrier based SVPWM allow fast and efficient implementation of SVPWM without sector determination. The technique is based on the duty ratio profiles that SVPWM exhibits. By comparing the duty ratio profile with a higher frequency triangular carrier the pulses can be generated, based on the same arguments as the sinusoidal pulse width modulation.

4.2.5 Fuzzy Logic Controller

The database of a rule-based system may contain imprecisions which appear in the description of the rules given by the expert. Because such an inference cannot be made by the methods which use classical two valued logic or many valued logic, Zadeh in (Zadeh, 1975) and Mamdani in (Mamdani, 1977) suggested an inference rule called "compositional rule of inference". Using this inference rule, several methods for fuzzy reasoning were proposed. Zadeh (Zadeh, 1979) extends the traditional Modus Ponens rule in order to work with fuzzy sets, obtaining the Generalized Modus Ponens (GMP) rule.

An important part of fuzzy reasoning is represented by Fuzzy Logic Control (FLC), derived from control theory based on mathematical models of the open-loop process to be controlled. Fuzzy Logic Control has been successfully applied to a wide variety of practical problems: control of warm water, robot, heat exchange, traffic junction, cement kiln, automobile speed, automotive engineering, model car parking and turning, power system and nuclear reactor, on-line shopping, washing machines, etc.

Fuzzy Logic is basically a multi-valued logic that allows intermediate values to be defined between conventional evaluations like yes/no, true/false, good/bad, etc. Notions like 'rather high' or 'quite low' can be formulated mathematically and processed by computers. In this way an attempt is made to apply a more human-like way of thinking in the programming of computers. Fuzzy logic is an alternative to traditional notions of set membership and logic.

4.2.6 Fuzzy Inference System

A fuzzy inference system (FIS) is a system that uses fuzzy set theory to map inputs (*features* in the case of fuzzy classification) to outputs (*classes* in the case of fuzzy classification).

An example of a Mamdani inference system is shown in Figure 5. To compute the output of this FIS given the inputs, one must go through six steps:

1. Determining a set of fuzzy rules

2. Fuzzifying the inputs using the input membership functions,

3. Combining the fuzzified inputs according to the fuzzy rules to establish a rule strength,

4. Finding the consequence of the rule by combining the rule strength and the output membership function,

5. Combining the consequences to get an output distribution, and

6. Defuzzifying the output distribution (this step is only if a crisp output (class) is needed).

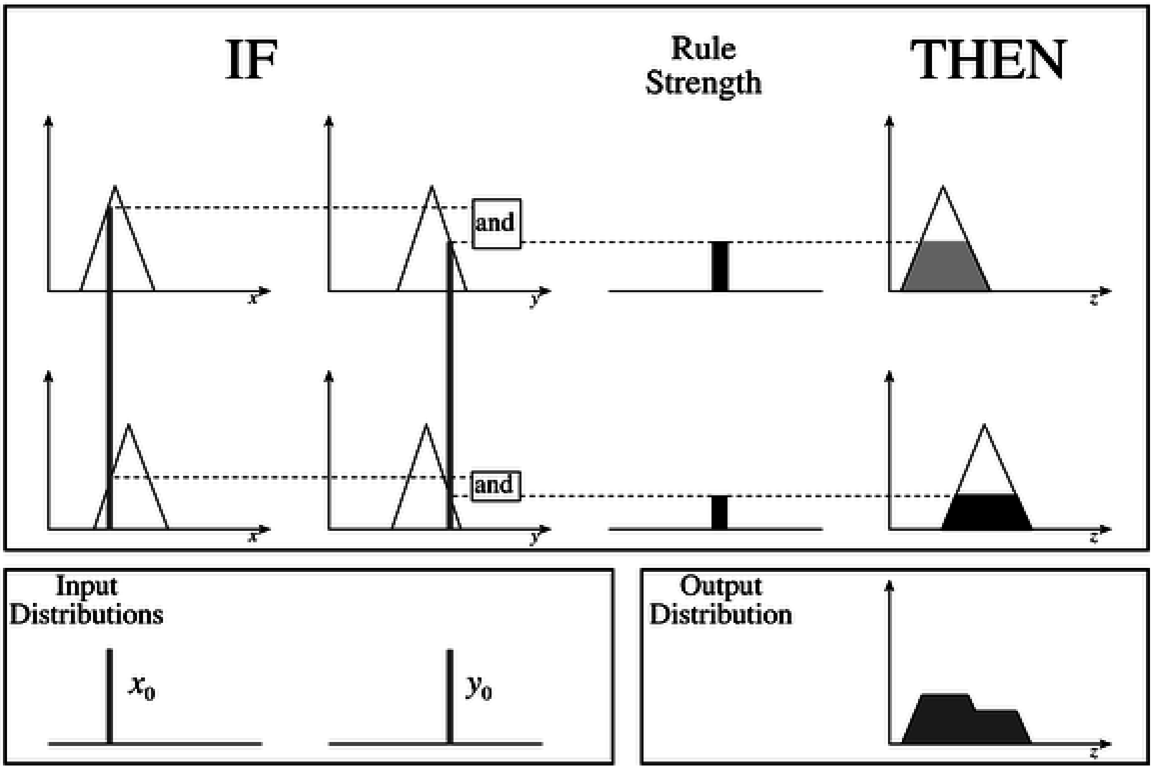

Figure 4.14: Fuzzy inference system

4.3 Conclusion

This chapter introduces classification of controlling techniques of induction motor drive and each technique has been discussed separately. It is concluded that vector control gives the good dynamic response as compared to scalar control. Also, between direct vector control and indirect vector control, indirect vector control is good because it is somewhat easy to implement and reference values are generated in feed forward manner. Further, two PWM techniques have been discussed i.e. hysteresis current controller and SVPWM (Space Vector PWM). Both techniques will be implemented in the simulation and results will be compared. Also, two controllers i.e. PI controller and Fuzzy Logic Controller will be implemented and compared.

CHAPTER 5
EFFICIENCY OPTIMIZATION OF THREE PHASE INDUCTION MOTOR

5.1 General

Induction motors are widely used in domestic, commercial and industrial application. Hence, they consume a major part of the total electrical energy production. Therefore, improving the efficiency of the induction motor is always been a major concern. Various essential strategies are adopted to ensure optimum efficiency operation of induction motor drive. This is usually realized either by selecting proper control strategies or by improvement in the design, materials and construction techniques or both. Design aspects involve shaping of rotor bars, use of copper material instead of aluminium, etc. As copper has high current density and low value of temperature coefficient as compared to aluminium. The control strategies adopted to optimize the efficiency are search controller and loss model controller. Search controller method is a feedback method that finds maximum efficiency by adopting a search technique. The value of efficiency at a particular sampling instant is compared with the efficiency value of previous sampling instant and necessary control action is executed accordingly. Further, back propagation method is also there in search algorithm. In case, the value of efficiency deteriorates in every new sampling instant then controller will back propagate and necessary control action will be taken from that point where efficiency is high. Hence, this method is slow but it is independent of motor parameters. Loss model controller depends on motor parameters because it is based on the modelling of the motor and losses to derive an objective function, which is optimized to yield maximum efficiency. It is a feed-forward method and treats the situation analytically by properly modelling the losses. Hence, this method is fast as compared to search controller. Machines are designed to operate at rated flux because if gives fast transient response and high torque to ampere ratio. If rated flux is maintained at light loads, then core losses of the machine will be excessively high which will result in reduced efficiency. Here, loss model control technique will be used to reduce the losses and increase the torque per ampere ratio by making rated flux as increasing function of load.

5.2 Efficiency Optimization Algorithm

The total losses of the motor consist of stator and rotor copper and core losses, friction losses, windage or unaccounted losses. The copper losses are mainly dependent on percentage of total load applied to motor and hence these losses can be given as:

$$P_{Cu} = \frac{3}{2}\left(i_{ds}^2 + i_{qs}^2\right)R_s + \frac{3}{2}\left(i_{ds}^2 + i_{qs}^2\right)R_r \quad 5.1$$

The iron losses due to eddy current and hysteresis losses are given by:

$$P_{Fe} = \frac{3}{2}(k_h\omega_e\Psi_m^2 + k_e\omega_e^2\Psi_m^2) \quad 5.2$$

Where,

$$\Psi_m^2 = \Psi_{dm}^2 + \Psi_{qm}^2 \quad 5.3$$

k_h - Hysteresis loss coefficient

k_e – Eddy current loss coefficient

Frictional losses are dependent on rotor speed and is given by:

$$P_{friction} = k_m\omega_r^2 \quad 5.4$$

Where,

k_m – Mechanical loss coefficient

The total losses can be expressed as:

$$P_{total} = \frac{3}{2}\left(i_{ds}^2 + i_{qs}^2\right)R_s + \frac{3}{2}\left(i_{ds}^2 + i_{qs}^2\right)R_r + \frac{3}{2}(k_h\omega_e\Psi_m^2 + k_e\omega_e^2\Psi_m^2) + k_m\omega_r^2 \quad 5.5$$

In rotor flux orientation,

$$\Psi_{dr} = \Psi_r$$

$$\Psi_{qr} = 0$$

Now substituting equations 3.22, 3.25 in 5.3 yields

$$\Psi_m^2 = L_m^2 i_{ds}^2 + \frac{L_m^2}{L_r^2}(L_r - L_m)^2 i_{qs}^2 \quad 5.6$$

$$P_{total} = \frac{3}{2}\left[\mathrm{x}(i_{ds}^2) + \mathrm{y}\left(\frac{T_e}{ki_{ds}}\right)^2\right] + k_m\omega_r^2 \qquad 5.7$$

$$x = R_s + (k_h\omega_e + k_e\omega_e^2)L_m^2 \qquad 5.8$$

$$\mathrm{y} = R_s + R_r\frac{L_m^2}{L_r^2} + (k_h\omega_e + k_e\omega_e^2)\frac{L_m^2}{L_r^2}(L_r - L_m)^2 \qquad 5.9$$

$$\mathrm{K} = \frac{3}{2}\frac{P}{2}\frac{L_m^2}{L_r} \qquad 5.10$$

To get minimum power loss, differentiate equation 5.7 with respect to i_{ds} and equating it to zero yields the optimal d-axis current:

$$\frac{dP_{total}}{di_{ds}} = \frac{3}{2}\left[2xi_{ds} - \left(\frac{T_e}{K}\right)^2\frac{2y}{i_{ds}^3}\right] = 0 \qquad 5.11$$

Thus,

$$i_{ds\ optimum} = \sqrt[4]{\frac{y}{x}\left(\frac{T_e}{K}\right)^2} \qquad 5.12$$

The optimum value of d- axis current is dependent on electromagnetic torque, since y, x, K are constant. Hence, the flux will vary according to the applied torque.

5.3 Conclusion

In this chapter, an efficiency optimization algorithm for induction motor drive has been developed. This control algorithm determined the optimal value of d- axis current to minimize the electrical losses of the machine for a particular speed and torque. This algorithm will be implemented in next chapter and results will be discussed.

CHAPTER 6

SIMULATION AND RESULTS

6.1 General

In this chapter, the dynamic performance of indirect vector controlled induction motor using different controllers is discussed. Firstly, the dynamic performance of induction motor using PI controller and Fuzzy logic controller have been implemented and compared. Further, the efficiency optimization algorithm that has been discussed in the previous chapter is implemented on vectored controlled motor using Hysteresis current controller (HCC), and results have been compared with constant flux vectored control method. Also, the same algorithm has been implemented on Space Vector PWM (SVPWM) instead of HCC. At last, the results have compared between two different controllers, i.e. SVPWM and HCC.

The indirect vector control has been implemented in MATLAB Simulink environment and it is performed on 1.1 KW, 50 Hz, 415 V, 146.67 rad/s induction motor drive. Also, the change in other parameters due change in set points of speed and torque have also been discussed.

6.2 Comparative study of indirect vector control of induction motor using PI controller and Fuzzy logic controller

The schematic diagrams of two controllers have shown in figure 6.1:

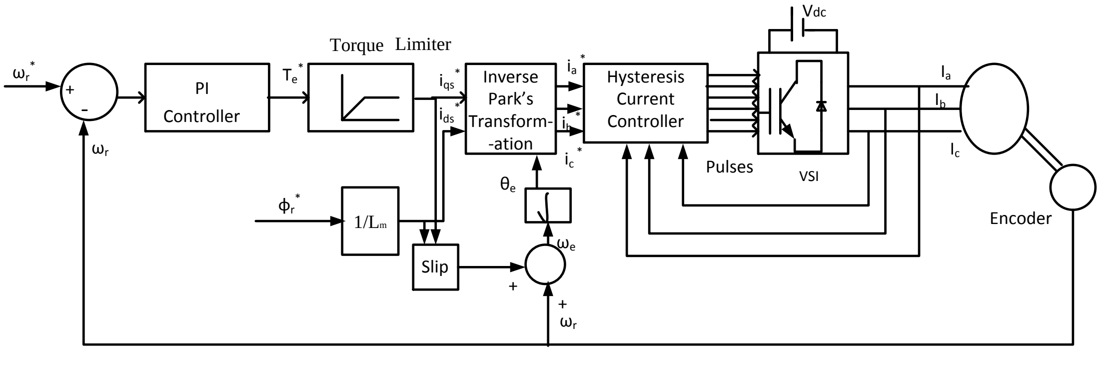

(a) Indirect vector control of induction motor using PI controller

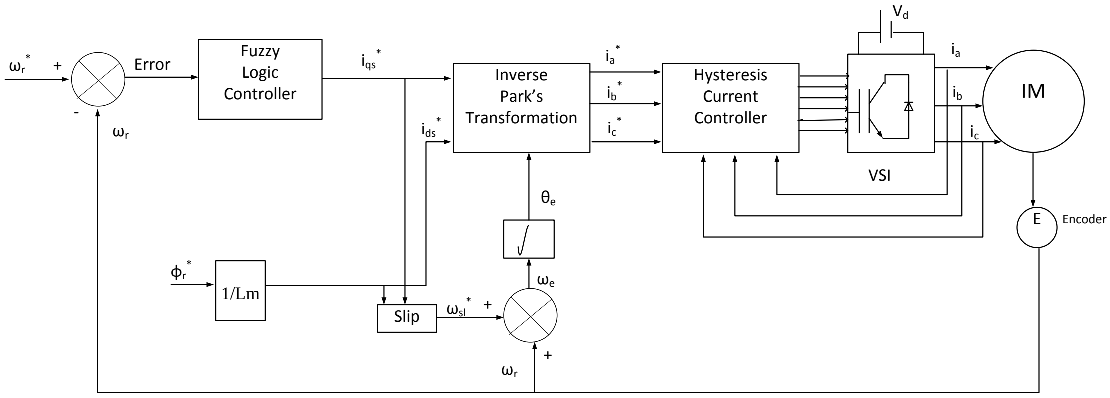

Figure 6.1(b): Indirect vector control of induction motor using FLC controller

Fuzzy logic controller take error in speed and change in error in speed as input and provide i_{qs}^{*} as output. The membership functions of two inputs and one output have been shown in figure 6.2:

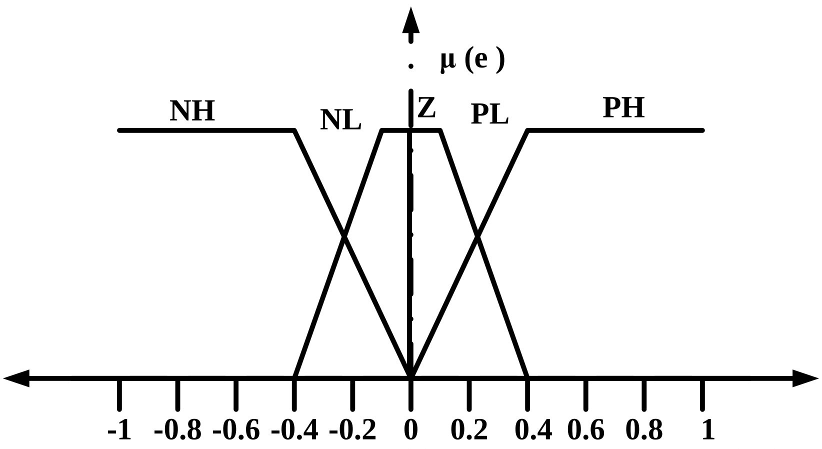

(a)

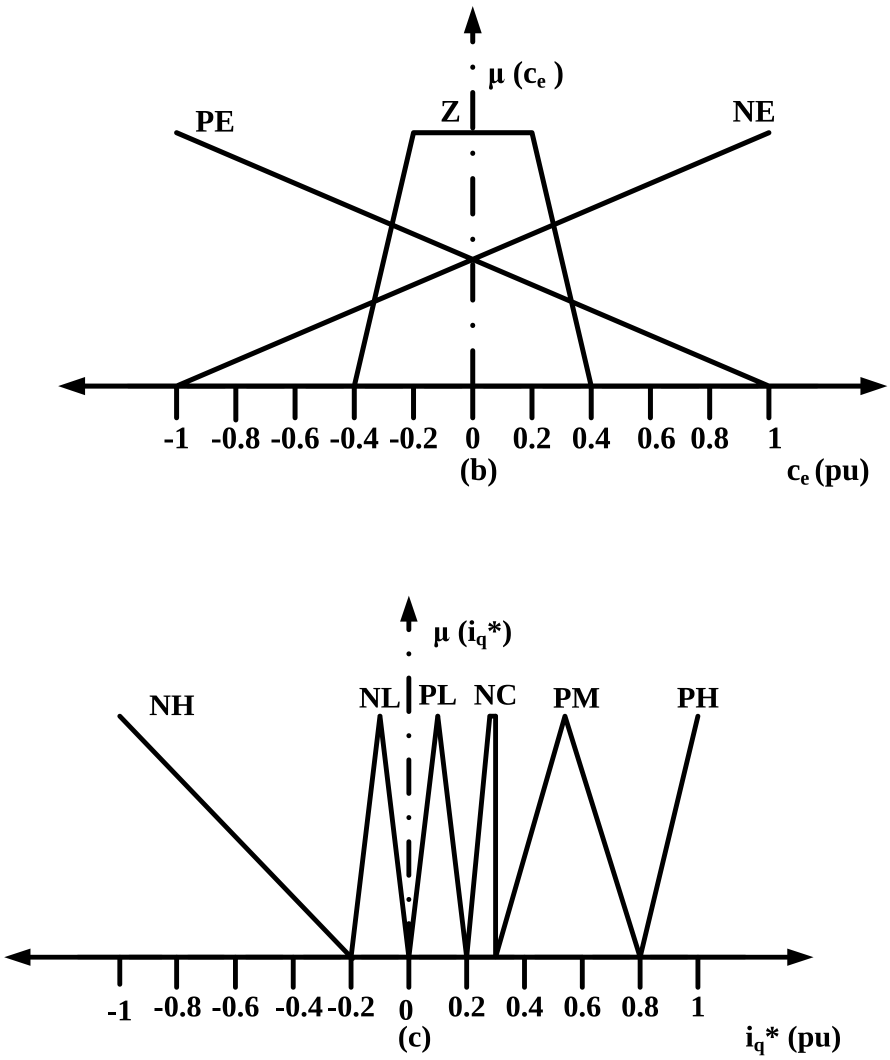

Figure 6.2: (a) Error in speed (p.u.) input variable membership function plots, (b) change in error in speed (p.u.) input variable membership function plot, (c) i_q^* (p.u.) output variable membership function plot.

The schematic representation of fuzzy logic controller is shown in figure 6.3.

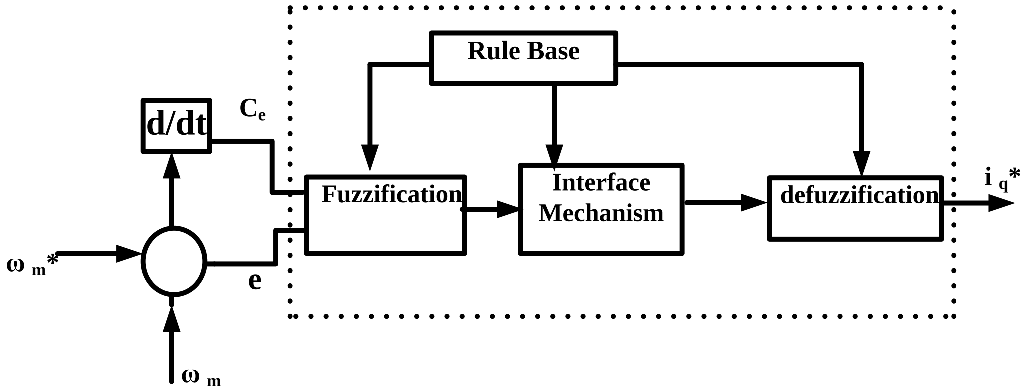

Figure 6.3: Fuzzy Logic Controller

The rule base for the concerned controller is:

1. If (e is PH) then (i_q^* is PH)
2. If (e is PL) then (i_q^* is PM)
3. If (e is Z) and (C_e is PE) then (i_q^* is PL)
4. If (e is Z) and (C_e is NE) then (i_q^* is NC)
5. If (e is Z) and (C_e is Z) then (i_q^* is NC)
6. If (e is NL) then (i_q^* is NL)
7. If (e is NH) then (i_q^* is NH)

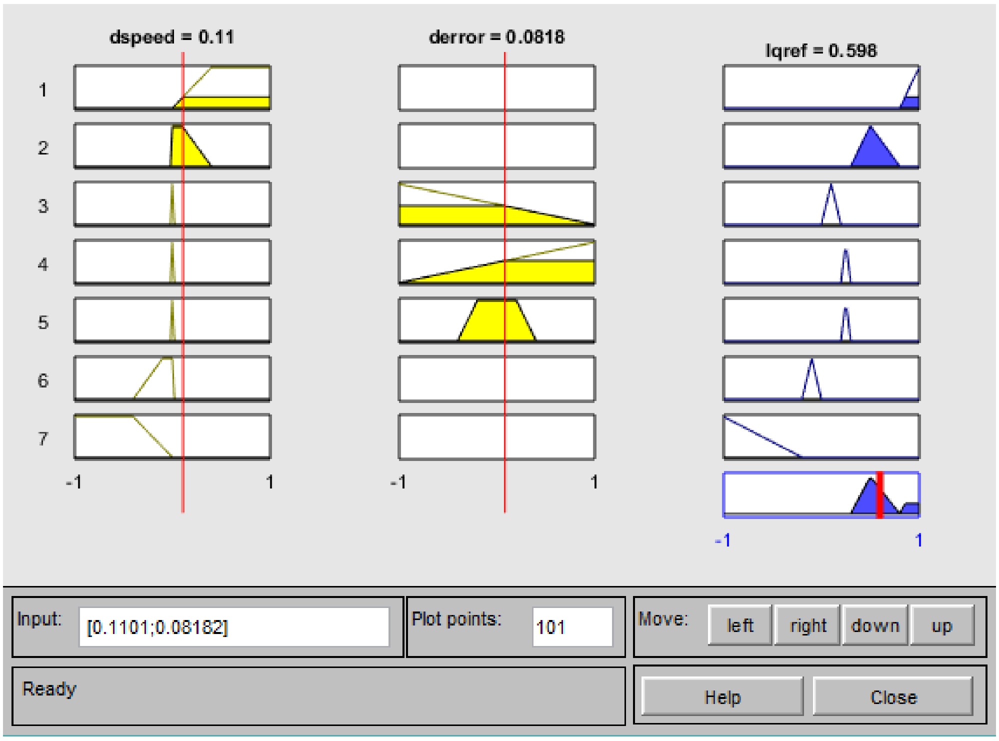

(a)

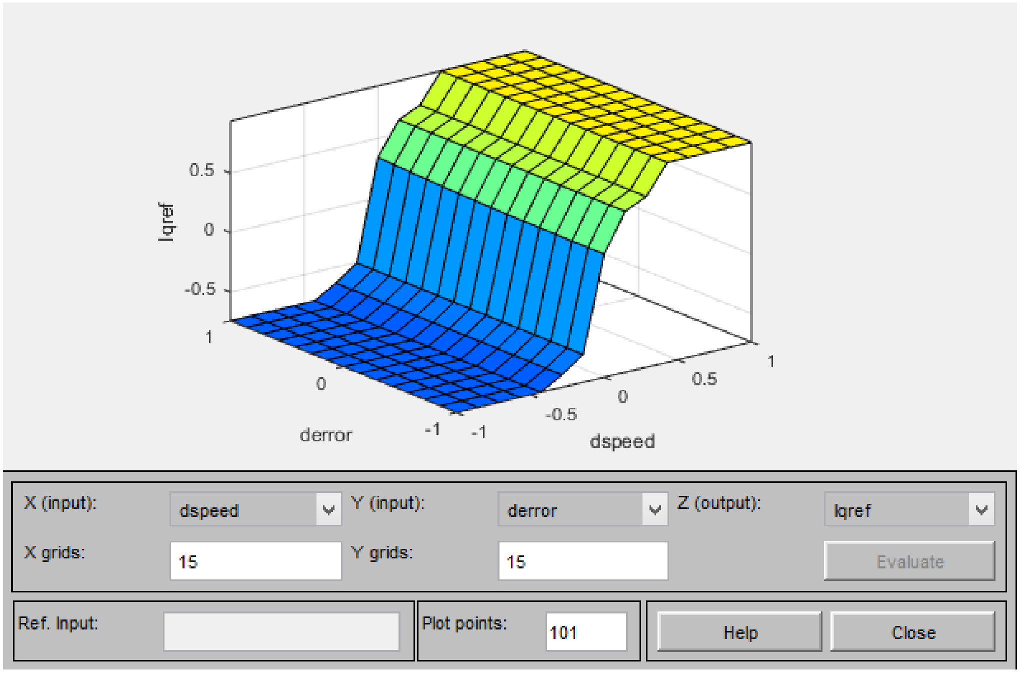

Figure 6.4(a): Rule Viewer, (b) Surface Viewer

The above Fuzzy logic design has been implemented in MATLAB/Fuzzy Logic Designer with FIS type Mamdani. The concerned Rule viewer at a particular condition and surface viewer has been shown in the figure 6.4. Here, e input variable is denoted as 'derror' and C_e input variable is denoted as 'dspeed' and i_q^* output variable is denoted as 'iqref'.

The simulation results have shown in figure 6.5:

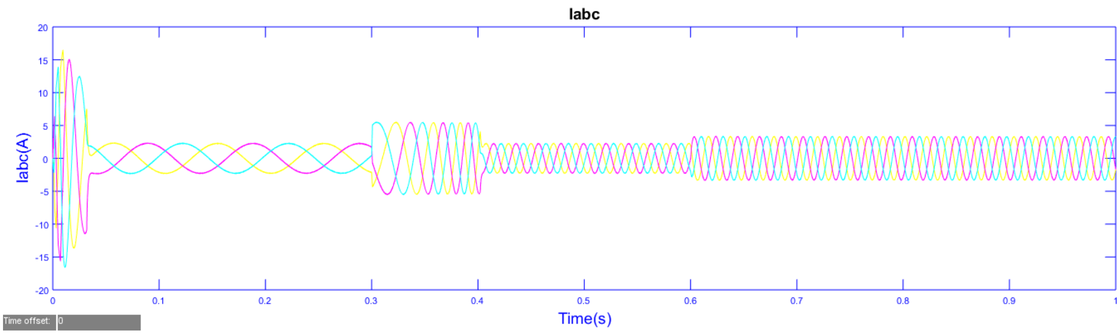

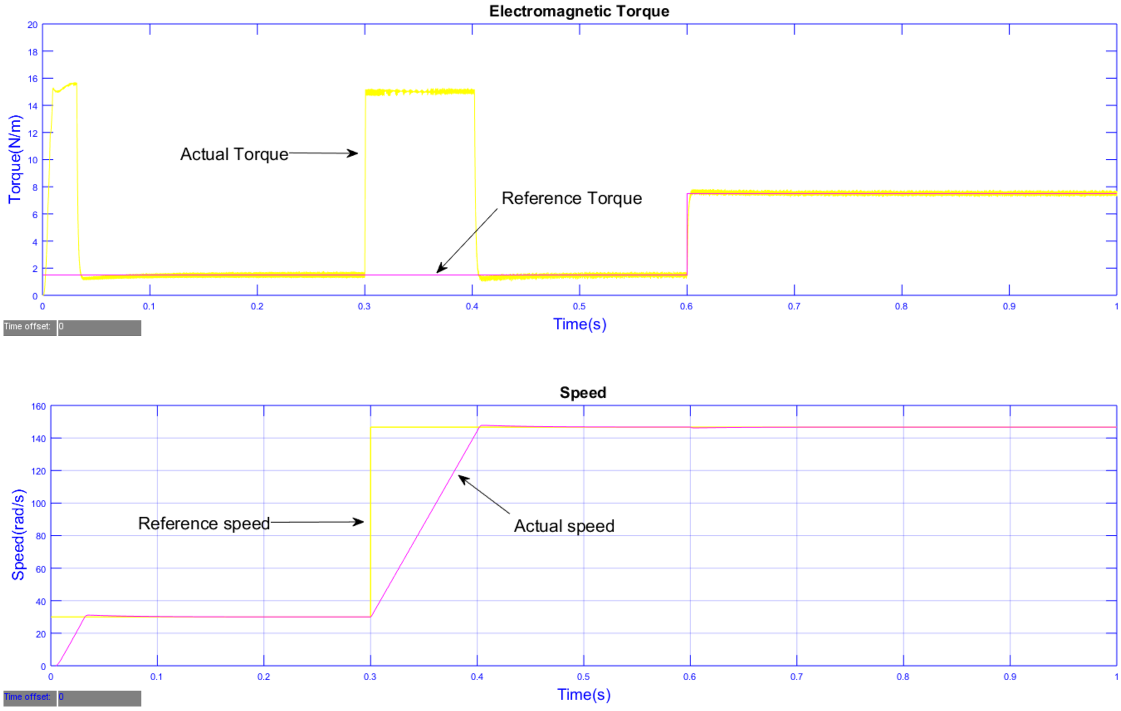

Figure 6.5(a): Dynamic Performance of induction motor using PI controller

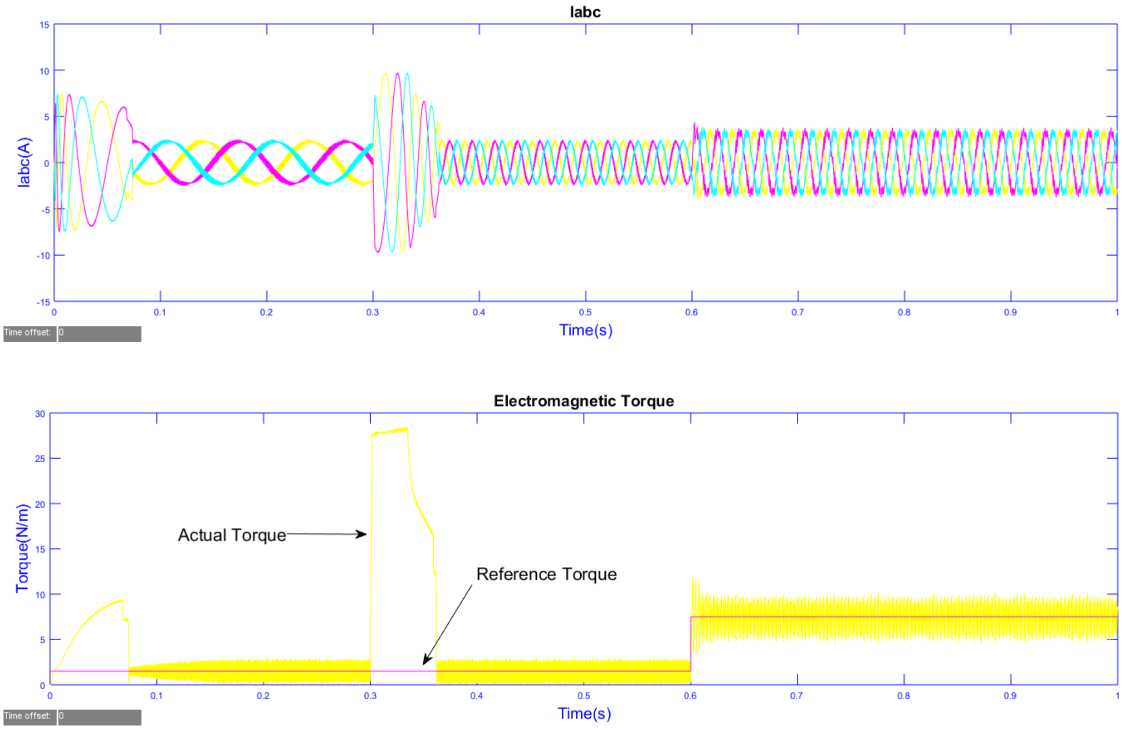

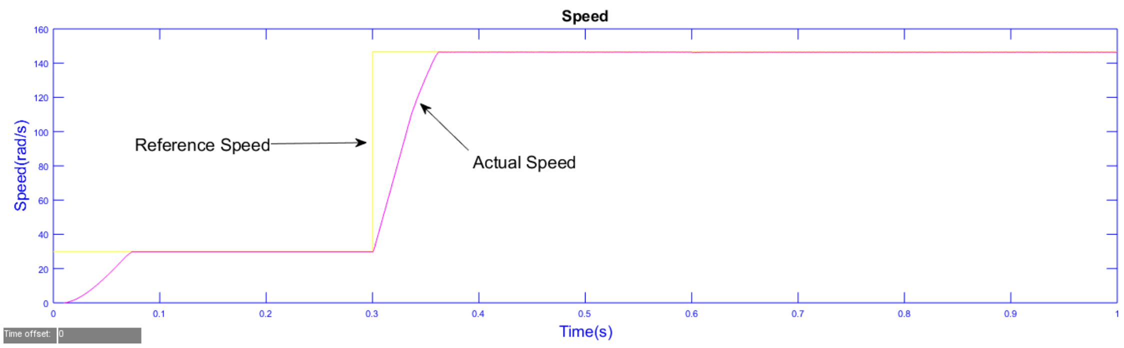

Figure 6.5(b): Dynamic Performance of induction motor using FLC controller

Initially the drive is started with a commanded speed of 29.33 rad/s (20% of rated speed) with load torque of 1.5 Nm (20% of rated torque). According to the results the conclusion can be drawn that dynamic performance of the induction motor in case fuzzy logic controller at starting is poor because the input values of error and change in error of speed of Fuzzy Logic Controller is less which generate slow changing value of i_q^* current according to the member functions and rule base implemented. Hence, motor takes more time (about 0.07 s) to reach 20% of rated speed from zero speed and current (I_{abc}) drawn by motor at starting is less in case of FLC method rather than conventional PI controller (it takes about 0.02 s). But, when motor reaches 20% of rated speed to rated speed (146.67 rad/s), the input values of error and change in error of speed is high which will generate high value of i_q^* current required to bring the motor to set speed. The variation of torque during this transient state is also high and similarly the current (I_{abc}) is high as compared to conventional method. Hence, motor takes less time to reach the rated speed in case of FLC method rather than PI controller. When torque is varied from 20% of rated torque to rated torque, there is no variation in dynamic speed of the motor in both the cases (i.e. PI controller and Fuzzy logic controller). This shows the decoupling effect due to vector control of induction motor. There exhibit no overshoot and undershoot in speed during transient response of fuzzy logic controlled induction motor. But, variation of torque around the set point in steady state is large in case of fuzzy logic controller as compared to PI controller.

6.3 Comparative study of indirect vector control of induction motor on applying and without applying efficiency optimization algorithm

The schematic representation of efficiency optimization of three phase induction motor has been shown below, figure 6.6:

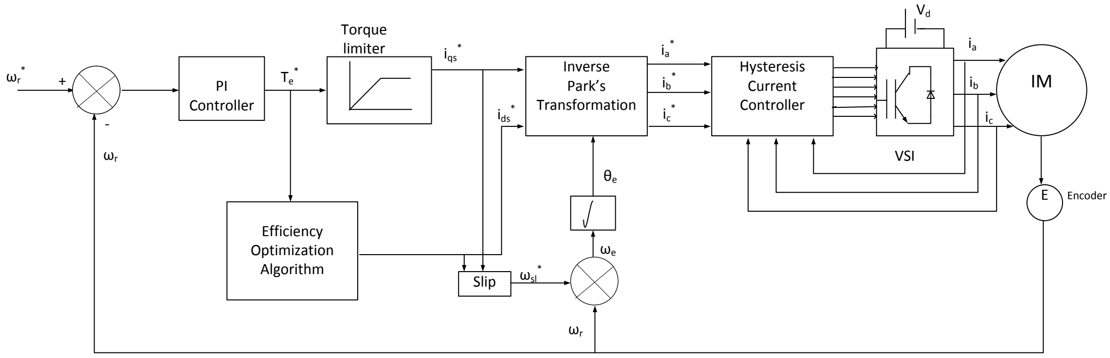

Figure 6.6: Schematic diagram of efficiency optimization algorithm

The simulated results have shown below, figure 6.7:

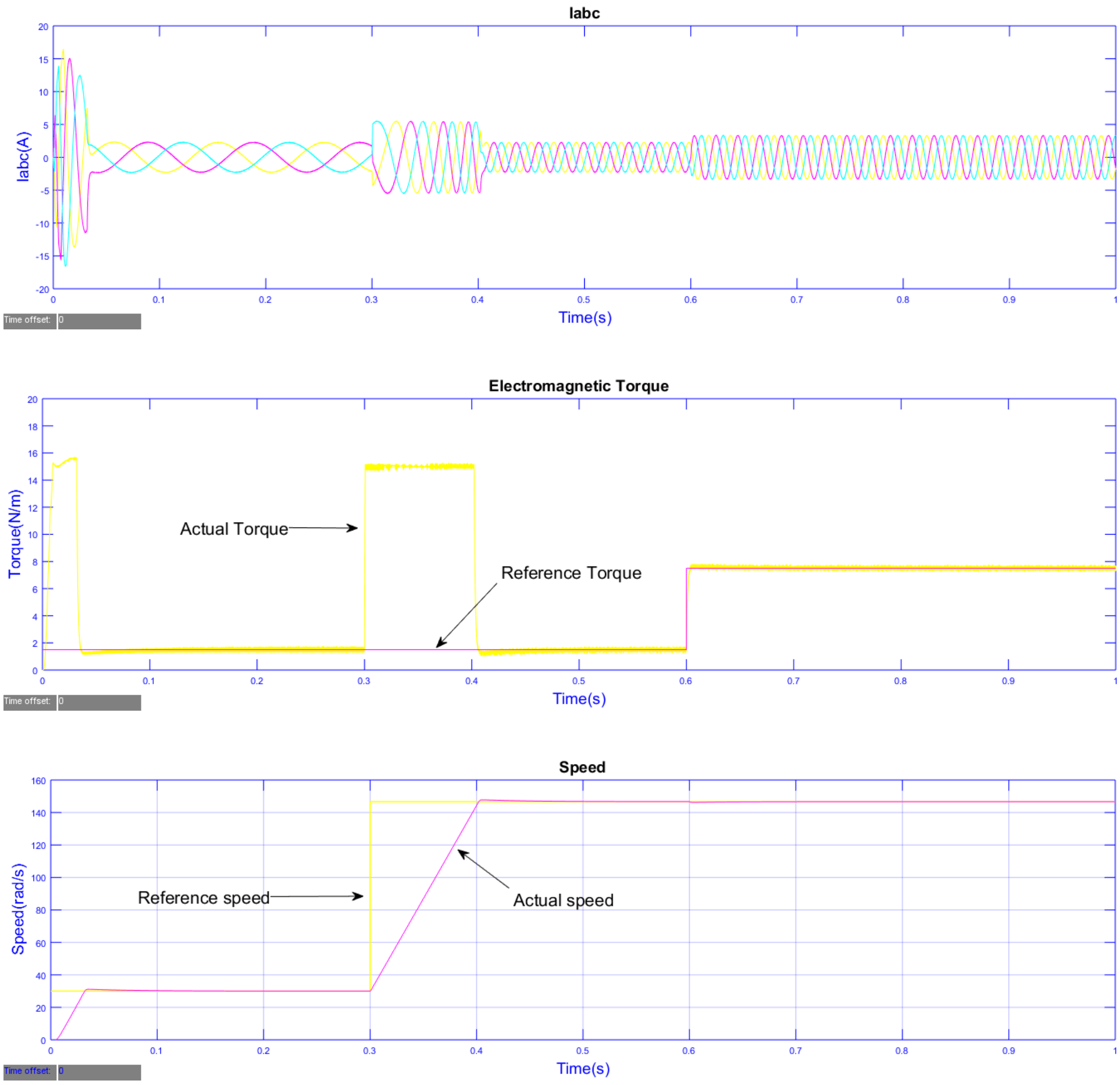

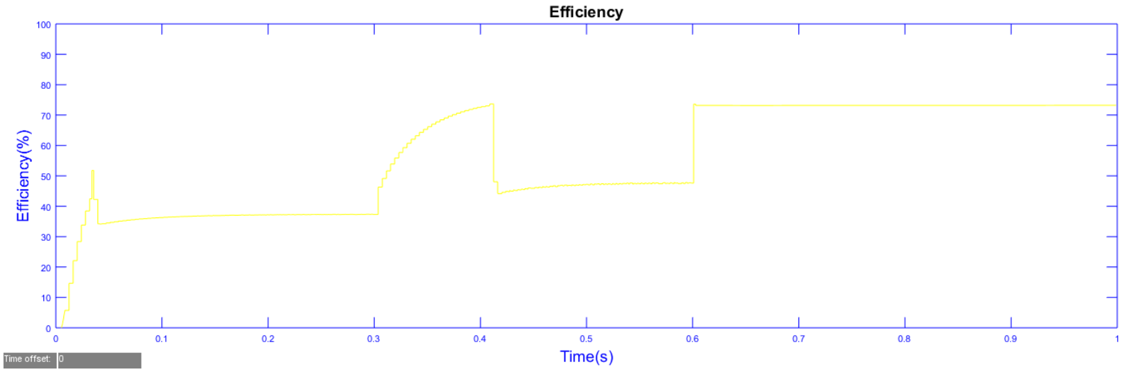

Figure 6.7(a): Dynamic performance of induction motor at constant reference flux

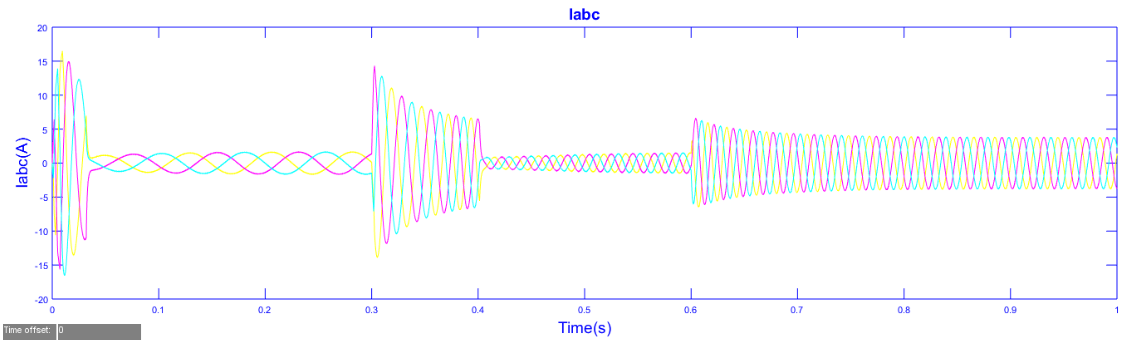

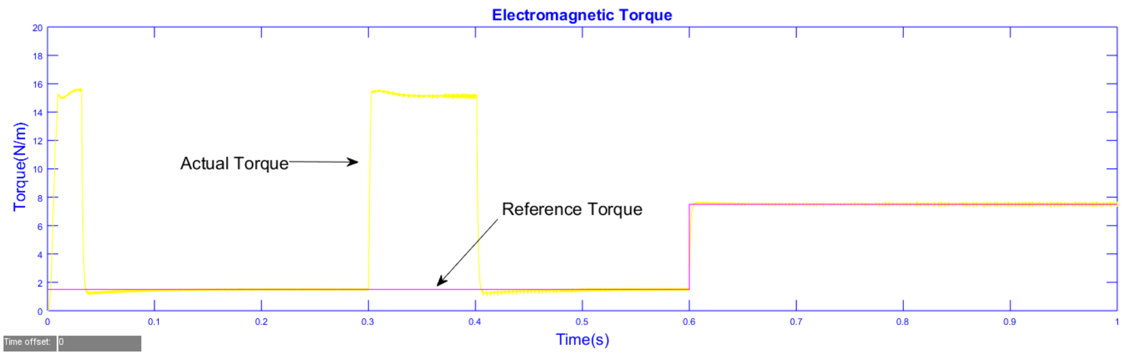

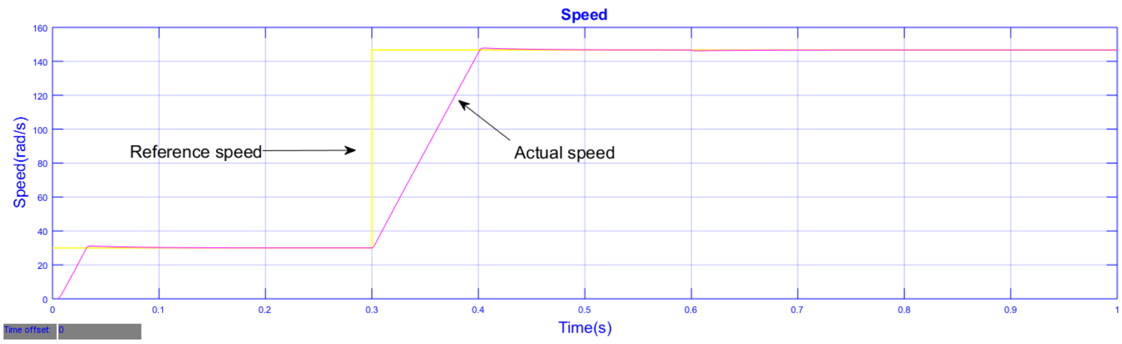

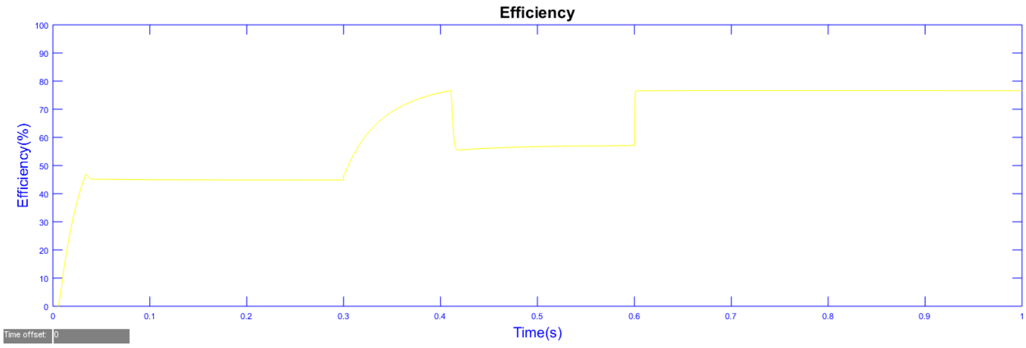

Figure 6.7(b): Dynamic performance of induction motor using efficiency optimization algorithm

Table 6.1: Performance parameters of induction motor 1.437 HP without optimization

Load(% of rated Torque)	**I_{ds} (p) (A)**	**I_{qs} (p) (A)**	**Cu Loss (W)**	**Fe Loss (W)**	**Mech Loss (W)**	**Total Loss(W)**	**η (%)**
Speed = 146.67 rad/s (rated speed)							
100	2.01	2.01	61	151.5	86	298.5	78.65
80	2.01	1.86	47	150	86	283	75.66
50	2.01	1.62	30	148	86	264	67.56
20	2.01	1.10	21	146	86	253	47.01
Speed = 117.34 rad/s (80% of rated speed)							
100	1.86	2.01	63	130	55	248	78.01
80	1.86	1.86	48	128.5	55	231.5	75.25
50	1.86	1.62	32	126	55	212	67.20
20	1.86	1.10	24	124	55	203	45.30
Speed = 73.33 rad/s (50% of rated speed)							
100	1.62	2.00	64	101	22	187	74.63
80	1.62	1.81	50	99	22	171	72.01
50	1.62	1.62	34	96.5	22	152.5	64.32
20	1.62	1.10	27	94	22	143	43.48
Speed = 29.33 rad/s (20% of rated speed)							
100	1.10	2.00	64	51	4	119	65.40
80	1.10	1.81	52	49	4	105	63.15
50	1.10	1.63	36	46	4	86	56.67
20	1.10	1.10	28	43	4	75	38.00

Table 6.2: Performance parameters of induction motor 1.437 HP with optimization

Load(% of rated Torque)	**I_{ds} (A)**	**I_{qs} (A)**	**Cu Loss (W)**	**Fe Loss (W)**	**Mech Loss (W)**	**Total Loss(W)**	**η (%)**
Speed = 146.67 rad/s (rated speed)							
100	2.03	2.03	61	149	86	296	78.80
80	1.88	1.88	51	127.2	86	264.2	76.90
50	1.63	1.63	35	95.75	86	216.75	71.73
20	1.20	1.20	26	52	86	164	57.30
Speed = 117.34 rad/s (80% of rated speed)							
100	2.02	2.02	63	128	55	246	78.15
80	1.88	1.88	58	118	55	231	75.30
50	1.63	1.63	32	85.6	55	172.6	71.82
20	1.20	1.20	24	64	55	143	55.10
Speed = 73.33 rad/s (50% of rated speed)							
100	2.02	2.02	63	91	22	176	75.76
80	1.88	1.88	52	83	22	157	73.70
50	1.62	1.62	34	65	22	121	69.50
20	1.10	1.10	27	50	22	99	52.63
Speed = 29.33 rad/s (20% of rated speed)							
100	2.02	2.02	64	42	4	119	67.14
80	1.88	1.88	52	35	4	91	66.52
50	1.63	1.63	36	30	4	70	61.65
20	1.10	1.10	28	19	4	51	46.87

Figure 6.7(a),(b) shows the simulated dynamic performance of the induction motor drive for sudden increase in speed and load torque without and with efficiency optimization respectively for 1.437 HP induction motor drive. Initially the drive is started with a command speed of 29.33 rad/s (20% of rated speed) with load torque of 1.5 Nm (20% of rated torque). During starting motor draws high stator current with low frequency to develop the necessary starting torque and once the motor picks up speed the frequency increases and magnitude of current reduces. There are small ripples in the stator current and hence in the developed electromagnetic torque due to switching in

hysteresis PWM current controller. At t = 0.3 s, when commanded speed is increased from 29.33 rad/s to 146.67 rad/s with the same load torque, the actual motor speed tracks the commanded speed. In addition, the torque does not change in steady state and there is no change in stator current. As, compared to conventional method, the efficiency of the motor is improved by almost 10% under this condition with optimization control. Similarly when load is increased from 20% to 100% of the rated torque at t = 0.6 s, the speed controller maintains the motor at rated speed. The electromagnetic torque developed by the motor increases to rated value 7.5 Nm to satisfy the load torque requirement with a proportional increase in stator current. Under rated speed and load operation, the improvement in efficiency with optimization control is less as compared to light load condition.

The graph between efficiency (%) and load torque (%) of the motor at rated speed (146.67 rad/s) is shown below:

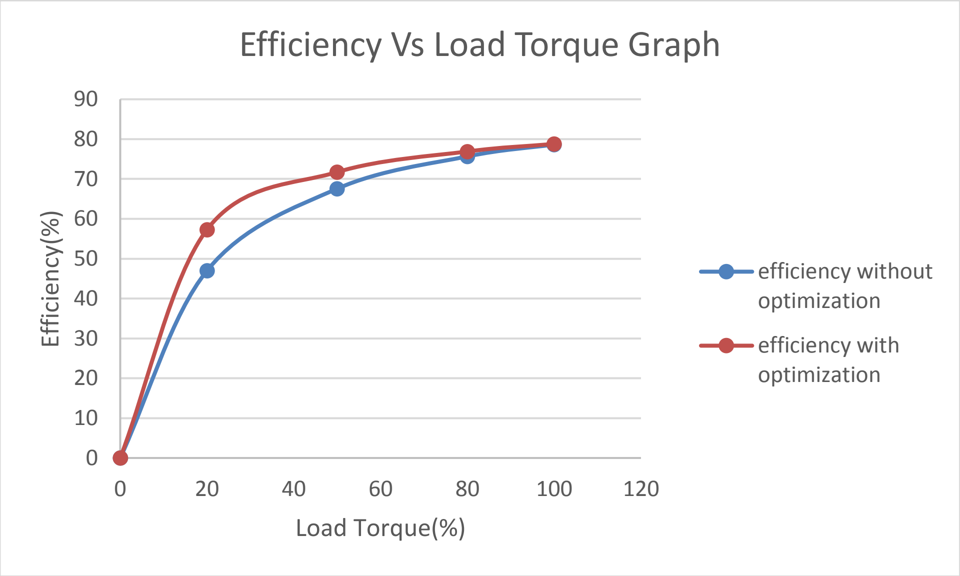

Figure 6.8(a) : Efficiency Vs Load Torque Graph

Similarly, the graph between the efficiency (%) and Speed (%) of the motor at 20% of the rated torque has been shown in the figure 6.8 (b).

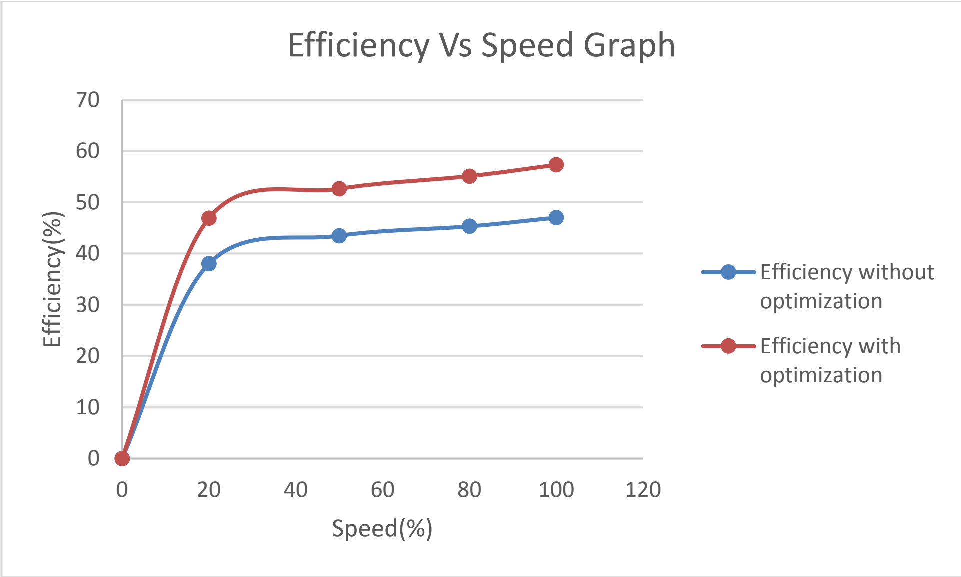

Figure 6.8 (b): Efficiency Vs Speed Graph

6.4 Efficiency optimization algorithm on indirect vector control method using SVPWM controller

The schematic representation of indirect vector control method using SVPWM controller using and without using efficiency optimization algorithm and concerned simulation results is shown in figure- 6.8

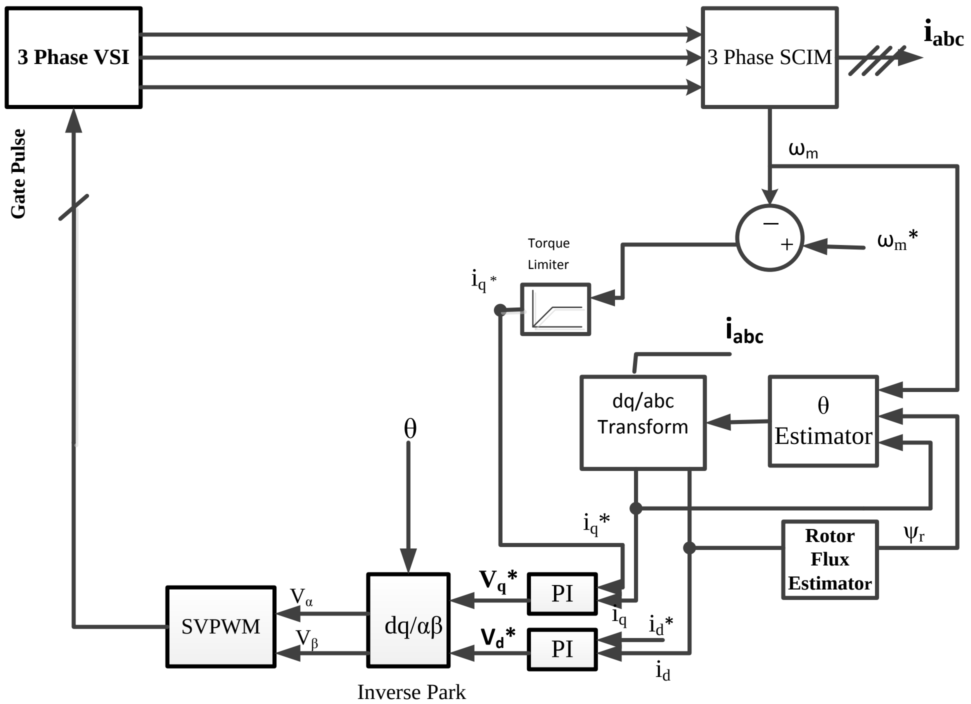

Figure 6.8(a): Schematic representation of indirect vector control method using SVPWM controller without using optimization algorithm.

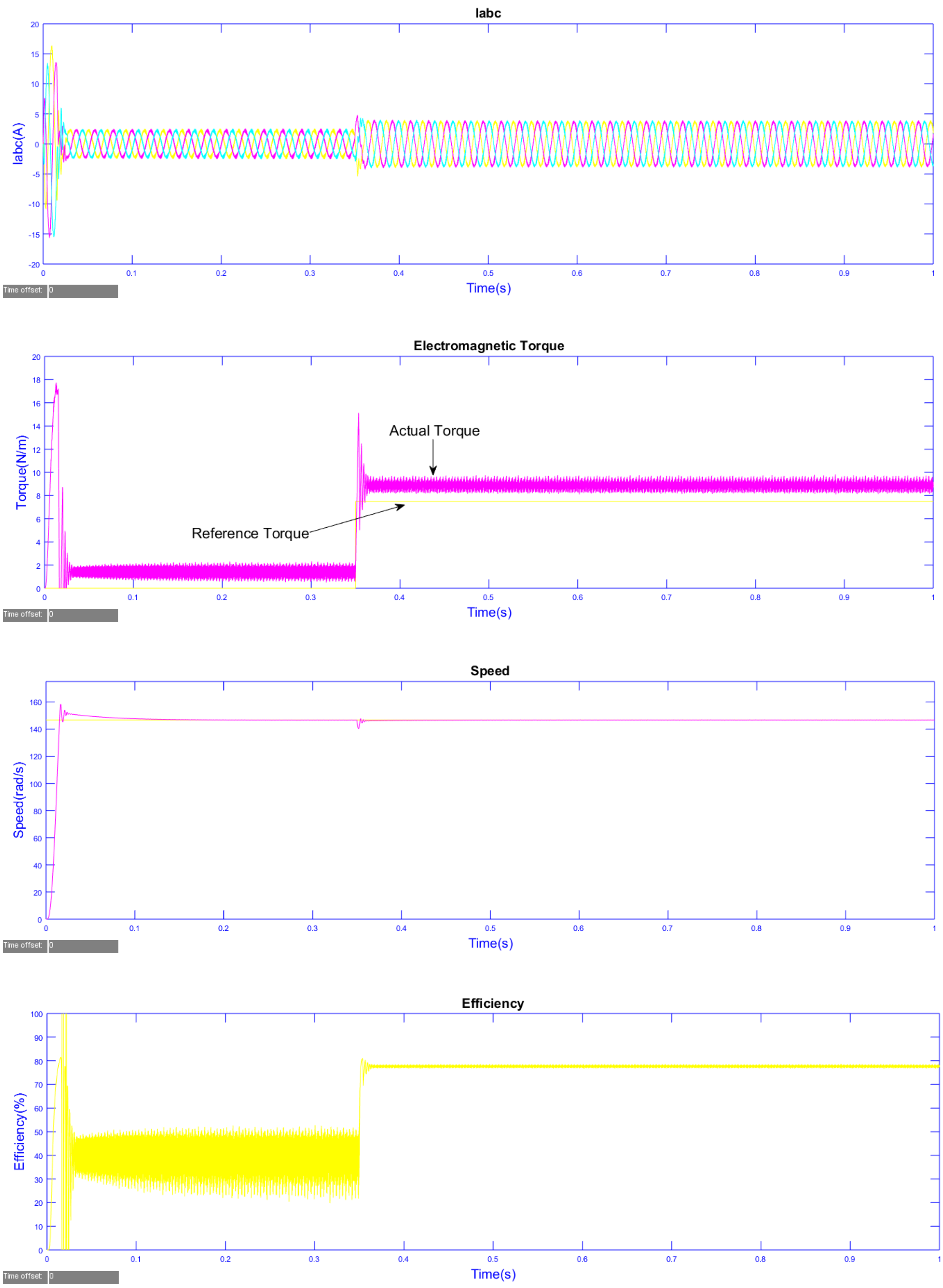

Figure 6.8(b): Dynamic performance of induction motor without using optimization algorithm

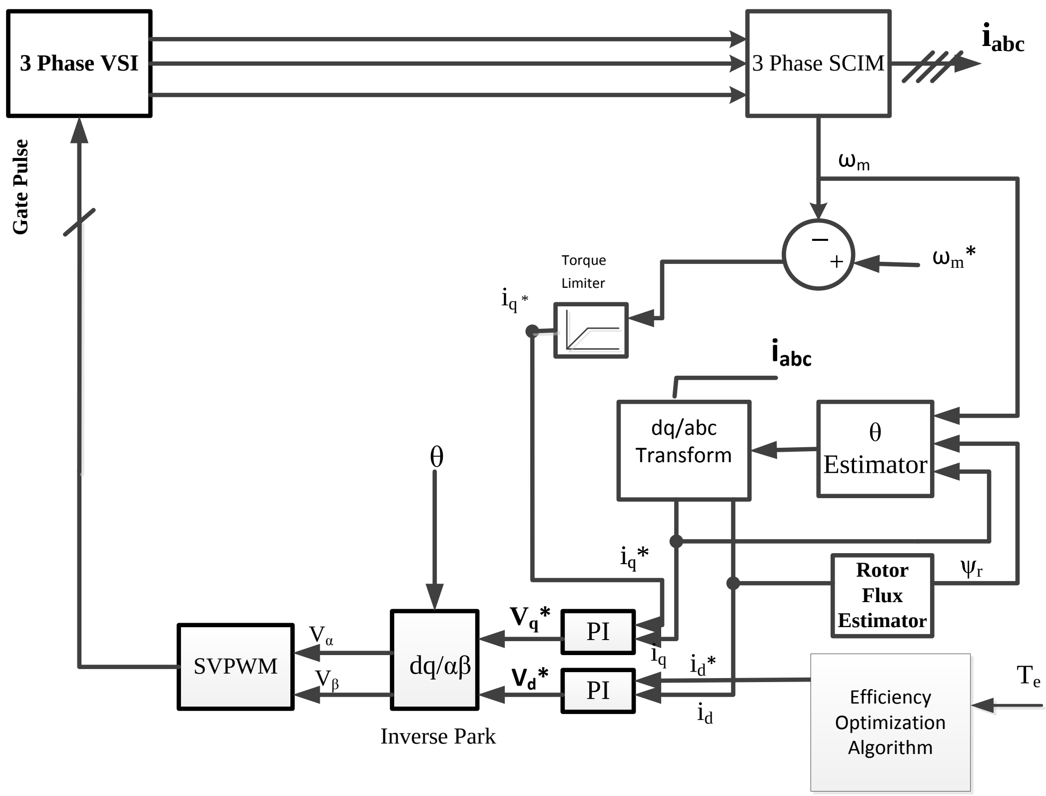

Figure 6.9(a): Schematic representation of indirect vector control method using SVPWM controller using optimization algorithm.

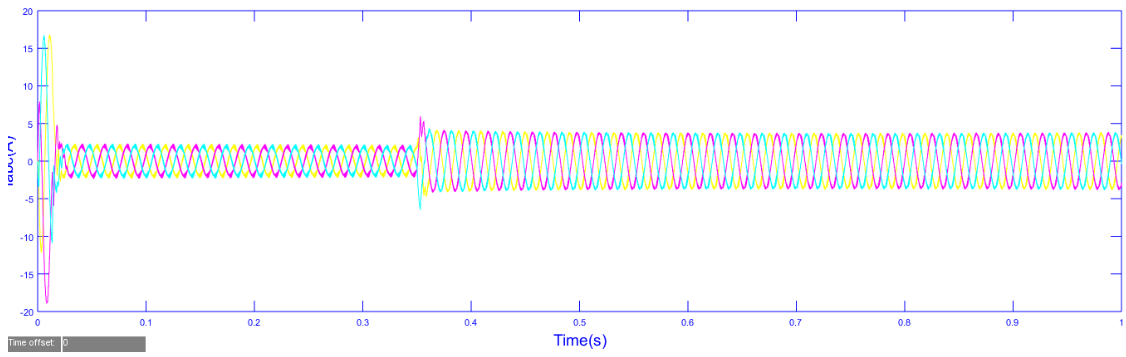

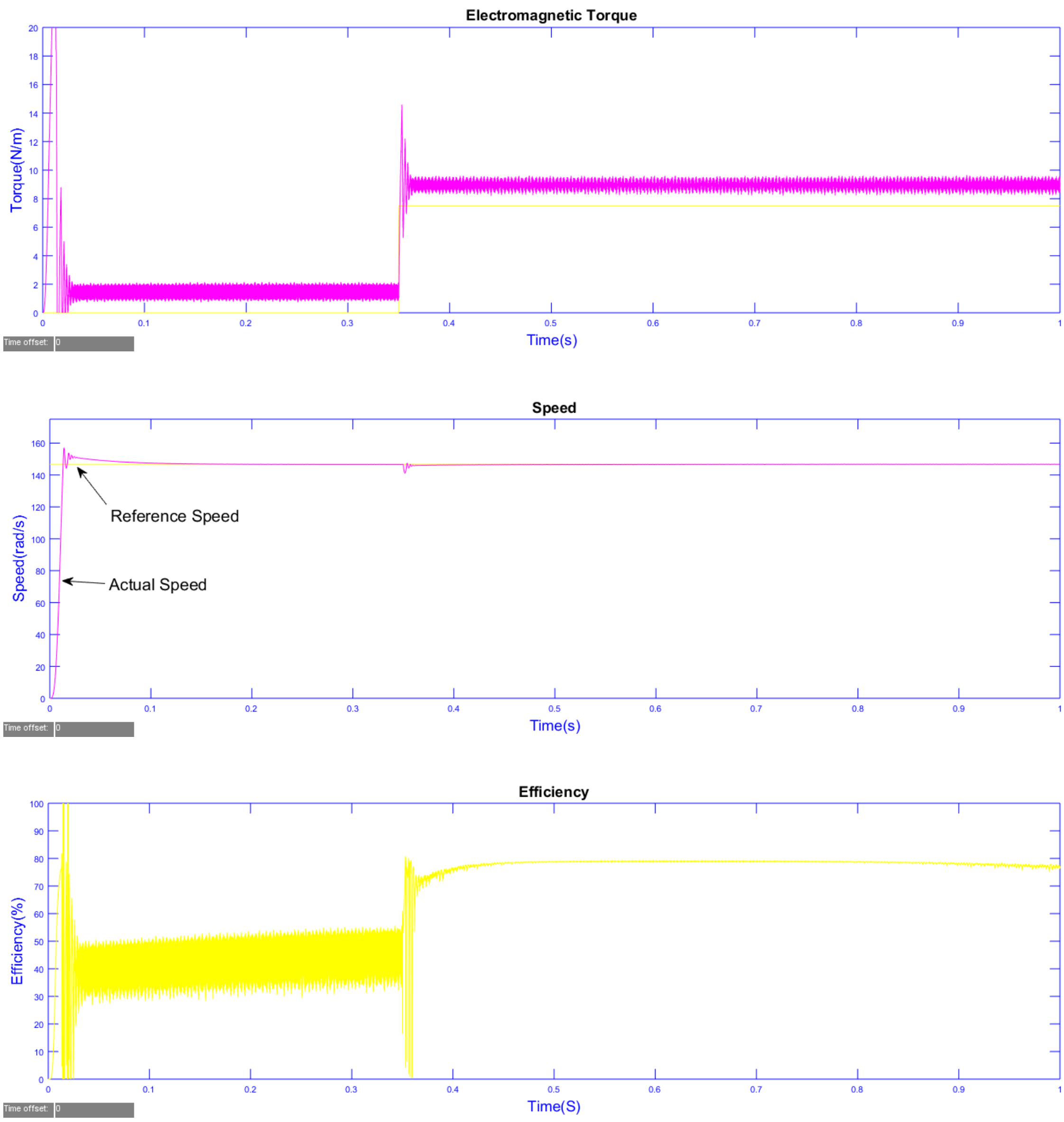

Figure 6.9(b): Dynamic performance of induction motor using efficiency optimization algorithm with SVPWM controller

From fig 6.9 and fig 6.10 show the simulated dynamic performance of the induction motor drive for sudden increase in load torque without and with efficiency optimization of algorithm respectively for 1.437 HP drive . Initially, the drive is started with a command speed of 146.67 (rated speed) with load torque of 1.5 Nm (20% of rated torque). Initially the motor draws high stator current to develop necessary starting torque and once the motor picks up the speed the magnitude of the current reduces. At t = 0.35 s, the load is increased from 20% to 100% of rated torque, the speed controller maintain the motor at rated speed. It is clear that efficiency of the motor is not optimized on using efficiency optimization algorithm because efficiency graph again roll back to low value. Hence, this loss model control does not work on SVPWM controller satisfactorily.

6.5 Conclusion

From above results, it is clear that on using fuzzy controller, there are no overshoots and undershoots. Hence, it results in good dynamic performance. Further, loss model control works well in hysteresis current controller compared to SVPWM. On using optimization algorithm, the efficiency of the motor is increased by 10% at low load (20% of the rated torque).

CHAPTER 7

CONCLUSION AND FUTURE SCOPE

7.1 Conclusion

The comparison between hysteresis current controller and SVPWM controller is presented for efficiency optimization of indirect vector controlled three phase IM drive. The dynamic performances of Induction motor drive using two different controllers show good performance and good stability for wide range of speeds with light load or full load. Hysteresis current control have faster response when compared with SVPWM technique as hysteresis current controller does not require large number of sampling. Also, loss model control gives good results on hysteresis current controller based model as compared to SVPWM controller based model. On using SVPWM controller, the efficiency remains same on using loss model controller.

7.2 Future Scope

Since, loss model control works satisfactorily with hysteresis current controller based model. Hence, this model can be implemented on other motors like permanent magnet synchronous machine and other ratings of induction motors. Further, two algorithms have been implemented. One is efficiency optimization algorithm that is implemented at steady state and during dynamic response like change in speed or load torque, the optimization algorithm is abandoned because that algorithm reduces the stator flux and constant flux value is applied for good dynamic response. When the response reaches to steady state, then controller is switched back to optimization algorithm after delay of few sampling instants.

REFERENCES

1. Michele Mengoni, Luca Zarri, Angelo Tani, Giovanni Serra and Domenico Casadei, "Stator Flux Vector Control of Induction Motor Drive in the Field Weakening Region." IEEE Trans.on Power Electronics, vol. 23, no. 2, pp. 941-949. March 2008.
2. Bimal K. Bose, Modern Power Electronics and AC drives, Low price edition, 2002.
3. Jun Zheng, Yunkuan Wang, Xiaofer Qin and Xin Zhang, "An offline Parameter Identification Method of Induction Motor, " in Proc of the 7th World Congress on Intelligent Control and Automotion WCICA 2008, pp. 8898-8901, Chongqing China. 25-27 Jun. 2008.
4. G.Estimaily, A Khodabakhshian and K. Jamshidi, "Vector Control of Induction Motors using UPWM Voltage Source Inverter,"1999, (available online),(Online) Available http://itee.uq.edu.au/aupec/aupec99/esmaily99.pdf..
5. Werner Leonhard. “Elements of reactor controlled reversible induction-motor drive,” Transaction of the American Institute of Electrical Engineers, Part 2,Vol. 78, pp. 106-115.
6. Werner Leonhard. “Adjustable Speech AC drives” Proceedings of the IEEE, Vol. 76, pp. 455 - 471.
7. Werner Leonhard. “Control of reversible induction motor drives,” Electrical Engineering, Vol. 78, pp. 905.
8. Hasan Zidan, Shuichi Fujii, Tsuyoshi Hanamoto and Teruo Tsuji,"A simple sensor less vector control system for valiable speed IM drives," Trans.IEEE japan.Vols.120-D,no.10,pp.1165-1170,2000.
9. H. Nejjari, M.E.H. Benbouzid: “ Application of fuzzy logic to induction motors condition monitoring” IEEE power engineering review, 1999, Vol. 19, pp. 52 – 54.
10. A. Munoz-Garcia, T.A. Lipo, D.W. Novotny: “A new induction motor v/f control method capable of high of high performance regulation at low speeds,” IEEE Transaction on industry application, Vol. 34, pp. 813-821.
11. Yen Shin Lai, Juo-Chiun Lin: “New hybrid fuzzy logic controller for direct torque control of induction motor drives,” IEEE Transaction on power electronics, 2003, Vol. 18, pp. 1211 – 1219.

12. Jee Hoon Jung, Gang- Youl Jeong, Bong- Hwan Kwon : “ Stability improvement of v/f controlled induction motor drive system by a dynamic current compensator,” IEEE Transaction on industrial electronics, 2004, Vol. 51, pp. 930-933.
13. Mohamed S. Zaky, Mohmoud M. Khater, Shokry S. Shokralla: “Wide speed range estimation with online parameter identification schemes of sensorless induction motor drives,” IEEE Transaction on Industrial electronics, 2009, Vol. 56, pp. 1699-1707.
14. J. Guzinski, H. Abu-Rub, H.A. Taliyat, “An advanced low cost sensorless induction motor drives,” IEEE Transaction on industry Application, 2003, Vol. 39, pp. 1757- 1764.
15. H.M. Kojadi, Liuchen Chang, R. Doraiswami: “ A MRAS- based adaptive pseudo reduced order flux observer for sensorless induction motor drives,” IEEE Transaction on power electronics, 2015, Vol. 20, pp. 930-938.
16. Gianmario Pellegrino, Paolo Guglielmi, Eric Armendo, Radu Lustin Bojoi, “ Self commissioning algorithm for inverter non linearity compensation in sensorless induction motor drive,” IEEE Transaction on industrial application, 2010, Vol. 46, pp. 1416-1424.
17. H. Benderradji, A. Benamer, L. Chrifi Alaoui, P. Bussy: “ Second order sliding mode induction motor control with a new Lyapunov approach,” 9 International multi conference, 2012, pp. 1-6.
18. F. . Lin, P. . Shen, and S. . Hsu, "Adaptive backstepping sliding mode control for linear induction motor drive," IEE Proceedings - Electric Power Applications, vol. 149, no. 3, p. 184, 2002..
19. M.-H. Park and K.-S. Kim, "Chattering reduction in the position control of induction motor using the sliding mode," IEEE Transactions on Power Electronics, vol. 6, no. 3, pp. 317–325, Jul. 1991.
20. S. Xepapas, A. Kaletsanos, F. Xepapas, and S. Manias, "Sliding-mode observer for speed-sensorless induction motor drives," IEE Proceedings - Control Theory and Applications, vol. 150, no. 6, pp. 611–617, Nov. 2003.
21. M. Cirrincione and M. Pucci, "An MRAS-Based Sensorless high-performance induction motor drive with a predictive Adaptive model," IEEE Transactions on Industrial Electronics, vol. 52, no. 2, pp. 532–551, Apr. 2005.

22. Y. B. Zbede, S. M. Gadoue, and D. J. Atkinson, "Model predictive MRAS Estimator for Sensorless induction motor drives," IEEE Transactions on Industrial Electronics, vol. 63, no. 6, pp. 3511–3521, Jun. 2016.
23. Toshiyuki Irisa, Sigeo Takata, Ryuzou Ueda and Toshikatsu Sonoda, "Reliability of Induction Machines for High Performance Based on Parameter Characteristics," IEEE Trans. Ind. Applications. Vols. IA-2, no. 2, pp. 414-421, Mar./Apr. 1985.
24. Vicente Leite, Rui Araujo and Diamantino Freitas, "Flux and Parameters Indentification of Vector-Controlled Induction motors in the Rotor Reference Frame," in Proc. AMC 2002, pp. 263-268, Maribor, Slovenia, 2002.
25. Vicente Leite, Rui Araujo and Diamantino Freitas, "A New Online Identification Methodology," in IEEE Int. Electric Machines and Drives Conf. IEMDC'03., vol. 1, pp. 449-455, Madison, Wisconsin USA, 01-04 Jun, 2003.
26. Marlen Varnovitsky, “A Microprocessor-Based Control Signal Generator for a Three Phase switching Power Inverter,” IEEE Trans. On Ind. Applications, Vols.1A-19, no. 2, pp. 228-234, Mar/Apr. 1983.
27. IEEE Trans. On Ind. And General Applications, Vols. IGA, no. 2, pp 212-217, Mar./Apr. 1971.
28. R. Krishnan, Victor R. Stefanovic, and James F. Lindsay, “Control Characteristics of Inverter-Fed Induction Motor,” IEEE Trans. On Industry Application, Vols. 1A-19, no. 1, pp. 94-104, Jan/Feb. 1983.
29. Robert T. Novotnak, John Chiasson and Mare Bodson, "High-Performance Motion Control of an Induction Motor with magnetic Saturation" IEEE Trans. on Control Systems Technology, vol.7,no.3,pp.315-327, May 1999.
30. "Speed Sensor less Vector Control of Induction Motor using Extended Kalman Filter," in Conf. Rec. of the 1992 IEEE Ind, Applications Society Anne Meetings, vol.1, pp.594-599: Houstan, Texas, USA, 04-09 Oct, 1992.
31. "Speed Sensor less” IEEE Trans, Ind, Applications vol.30, no.5, pp.1225-1233, Oct. 1994.
32. in Proc. The 5th Int. Conf. on Power Electronics and Drive Systems, 2003. PEDS '03, pp. 423-426, 2003.
33. IEEE Trans. on Ind. Application, vol.28, no. 5, p.1054-1061, Sep/Oct. 1992.

34. Geng Yang and Tung-Hai chin, "Adaptive-Speed Identification Scheme for a Vector-Controlled Speed Sensorless Inverter-Induction Motor Drive," IEEE Trans. on Ind. Application, vol. 29, no. 4, pp. 820-825, Jul/Aug.1993.
35. in Proc. of the 1995 21st IEEE Ind. Electronics, Control, and Instrumentation Conf, 1995, IECON'95,pp 524-529, 1995.
36. Teresa Orlowska, Mateusy Dybkowski, “Adaptive Sliding mode neuro fuzzy control of two mass induction motor drive,” IEEE transaction on industrial electronics, Vol. 57, pp. 553 – 564.
37. B.K. Bose and N.R. Patel, "A Sensorless Stator Flux Oriented Vector Controlled Induction Drive with Neuro-Fuzzy Based Performance Enhancement," in Conf. Rec. 1997 IEEE IAS Annu. Meeting. vol.I, pp. 393-400, New Orleans. Louisiana, USA.
38. Fabio Lima, Walter Kaiser, Ivan Nunes da Silva: “Speed Neuro Fuzzy Estimator applied to sensorless induction motor control,” IEEE transaction, 2012, Vol. 10, pp. 2065 – 2073.
39. M.N. Uddin, T.S. Radwani, M.A. Rahman: “Performances of fuzzy logic based indirect vector control of drive,” IEEE transaction on industry applications, 2002, Vol. 38, 1219-1225.
40. B. Karanayil, M.F. Rahman, C. Grantham : “Stator and rotor resistance observers for induction motor drive using fuzzy logic and artificial neural networks,” IEEE Transaction on Energy Conversion, 2005, Vol. 20, pp. 771-780.
41. Mini Sreejeth, Madhusudan Singh: “Efficiency optimization of vector controlled induction motor drive,” 2012 IEEE, pp. 1758 – 1763.
42. Daniel S. Krischen and Donald W. Novotny, "On-line Efficiency Optimization of a Variable Frequency Induction Motor Drive," IEEE Trans. Ind. Applications, vols. 1A-21, no. 4, pp. 610-616, May-Jun 1985.
43. Parviz Famouri and Jummie J. Cathey, "Loss Minimization control of an Induction Motor Drive," IEEE Trans. Ind. Applications, vol. 27, no. 1, pp. 32-37, Jan-Feb. 1991.
44. Gyu-Sik Kim, In Joong Ha, and Myoung-Sam Ko, "Control of Induction Motors for Both High Dynamic Performance and High Power Efficiency." IEEE Trans. Ind. Electronics. vol. 39. No. 4 p. 323-333, Aug. 1992.

45. Bimal K. Bose, Nitin R. Patel, and Kaushik Rajashekara, " A Neuro-Fuzzy-Based On-Line Efficiency Optimization Control of a Stator Flux-Oriented Direct Vector-Controlled Induction Motor," IEEE Trans. on Ind. Electronics, vol. 44, no. 2, pp. 270-273, April 1997.
46. G.O. Garcia, J.C. Mendes Luis, R.M. Stephan, and E.H. Watanabe, "An Efficient Controller for an Adjustable Speed Induction Motor Drive," IEEE Trans. Ind. Electronics, vol. 41, no. 5, pp. 533-539, Oct. 1994.
47. M. Waheedabeevi, Nithin S Nair, “New online loss minimization-based control of scalar and vector-controlled induction motor drives.” IEEE 2012 International Conference on Power Electronics, Drives and Energy Systems, pp. 1-7.
48. Junzi Yu, Wenhui Pei: “A Loss Minimization Port-Controlled Hamilton Scheme of Induction Motor for Electric Vehicles,” IEEE Transaction on Mechatronics, 2015, pp. 2465 – 2653.
49. Maria Carmela Di Piazza, Marcello Pucci: “Induction Machines Based Wind Generators with Neural Maximum Power Point Tracking and Minimum losses Techniques” IEEE Transaction on Industrial Electronics 2016, pp. 944 – 955, Volume: 63.
50. Srikanthan Sridharan, Philip T. Krien: “System level loss minimization of VSI based induction motor drives” IEEE 2015 International Electric Machines and Drives and Conference, pp. 1761 – 1767.
51. Srikanthan Sridharan, Philip T. Krien: “Induction motor drive design for traction application based on drive cycle energy minimization” IEEE 2014 Applied Power Electronics Conference and Exposition, pp. 1517 – 1521.
52. Faa-Jeng Lin and Wen-Der Chou, "An Induction Motor Servo Drive using Sliding-mode Controller with Genetic Algorithm, " Electric Power Systems Reserach Elsevier, vol. 64, pp. 93-108, 2003.
53. D. Grenier; L. -A. Dessaint; O. Akhrif; B. Le Pioufle: “Nonlinear torque control using the effect of salience in a synchronous motor” Canadian Conference, 1995, Vol. 1, pp. 300 – 305.
54. Olorunfemi Ojo, Ishwar Baht and Glenn Sugita, "Steady-state Optimization of Induction Motor Drives Operating in the Field Weakening Region," in Record 24th Annual IEEE Power Electronics Specialist Conf. 1993, Vol. 2, pp. 979-985, Seattle, Washington, USA, 1993.

APPENDIX –I

Table A.1 System Parameters

Rated Power	1.437 hp
Rated Voltage	415 V
Resistance of Stator	6.03 Ω
Inductance of Stator	0.5192 H
Resistance of Rotor	6.085 Ω
Inductance of Rotor	0.5192 H
Mutual Inductance	0.4893 H
Frequency	50 Hz
Rotor friction co-efficient	0.0027 Kgm^2/s
Motor Inertia	0.01178 kg m^2
Pole pairs	2
Rated Torque	7.5 Nm
Rated Speed	146.67 rad/s

APPENDIX – II

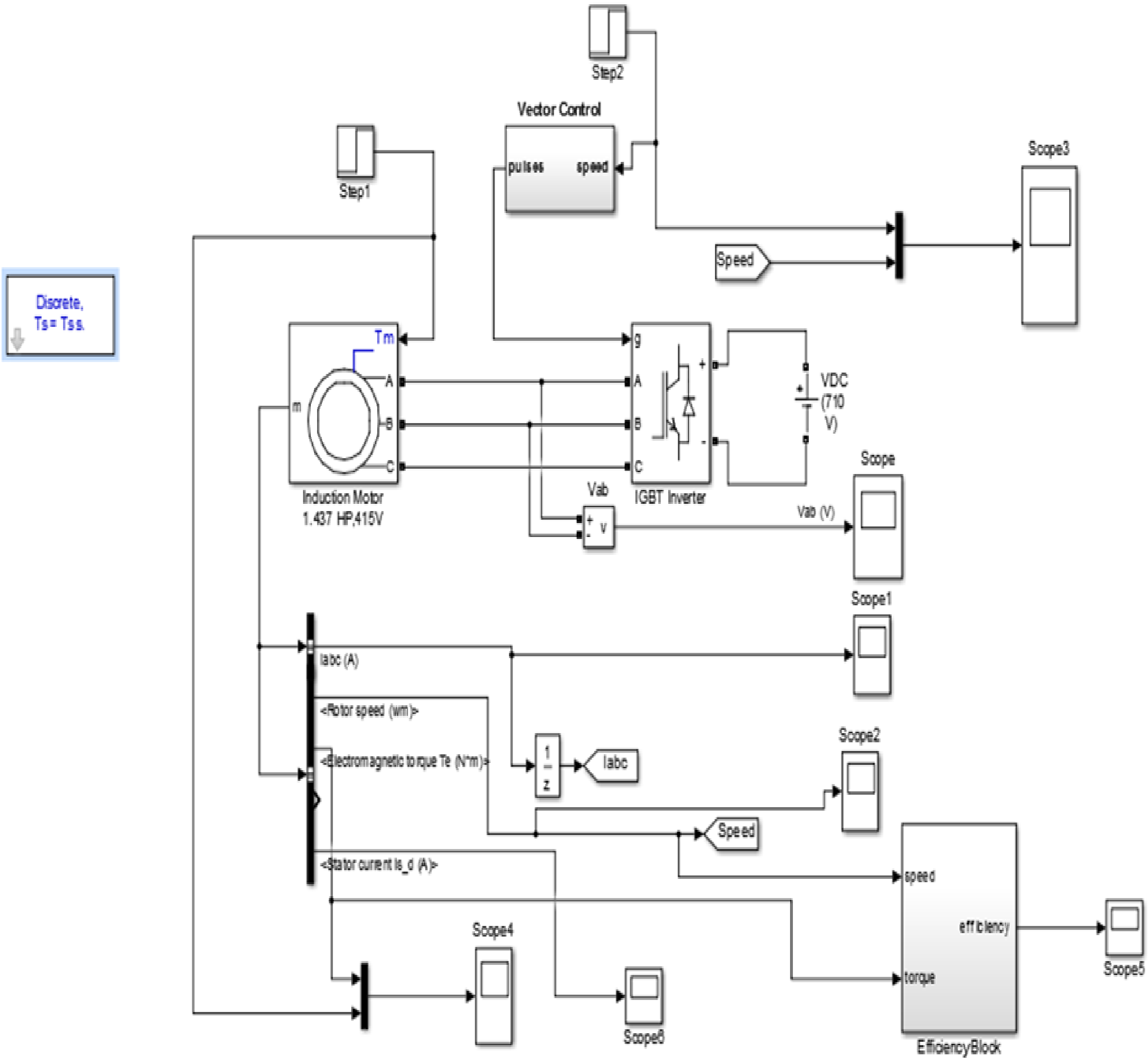

Figure A.1 A Simulink model for indirect vector control induction motor with PI controller using Hysteresis Current Controller for generating pulses

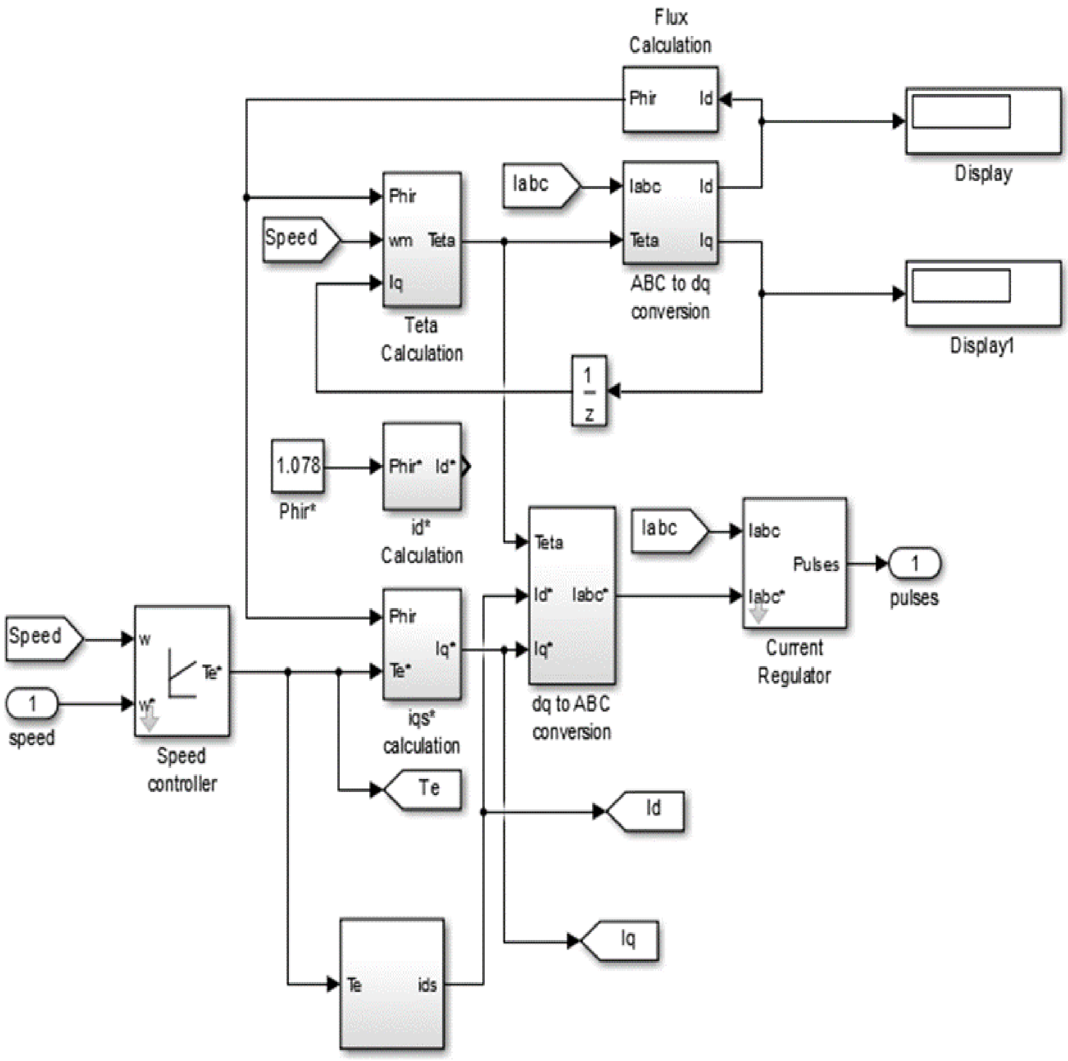

Figure A.2 Simulink model of indirect vector control for efficiency optimization

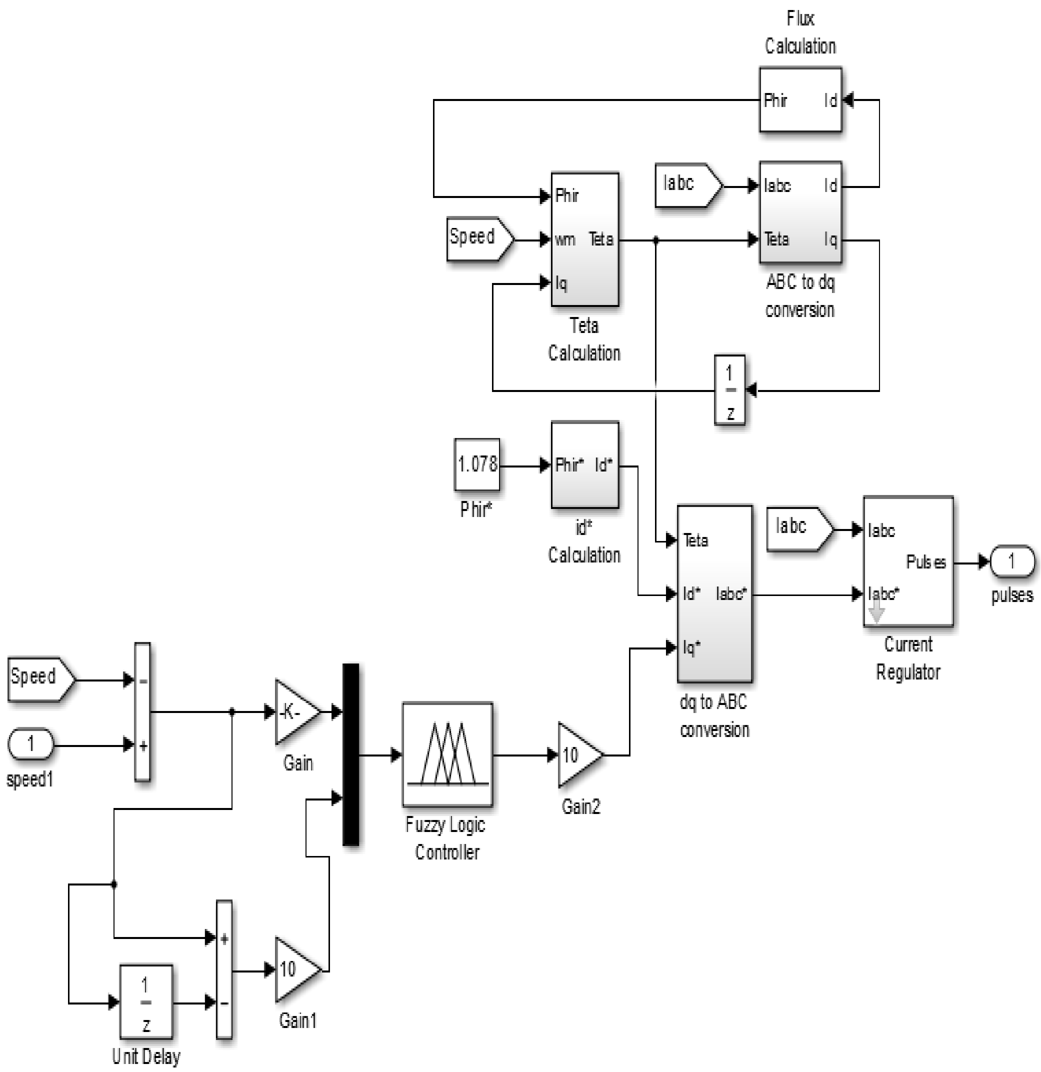

Figure A.3 Simulink model of indirect vector control using fuzzy logic controller

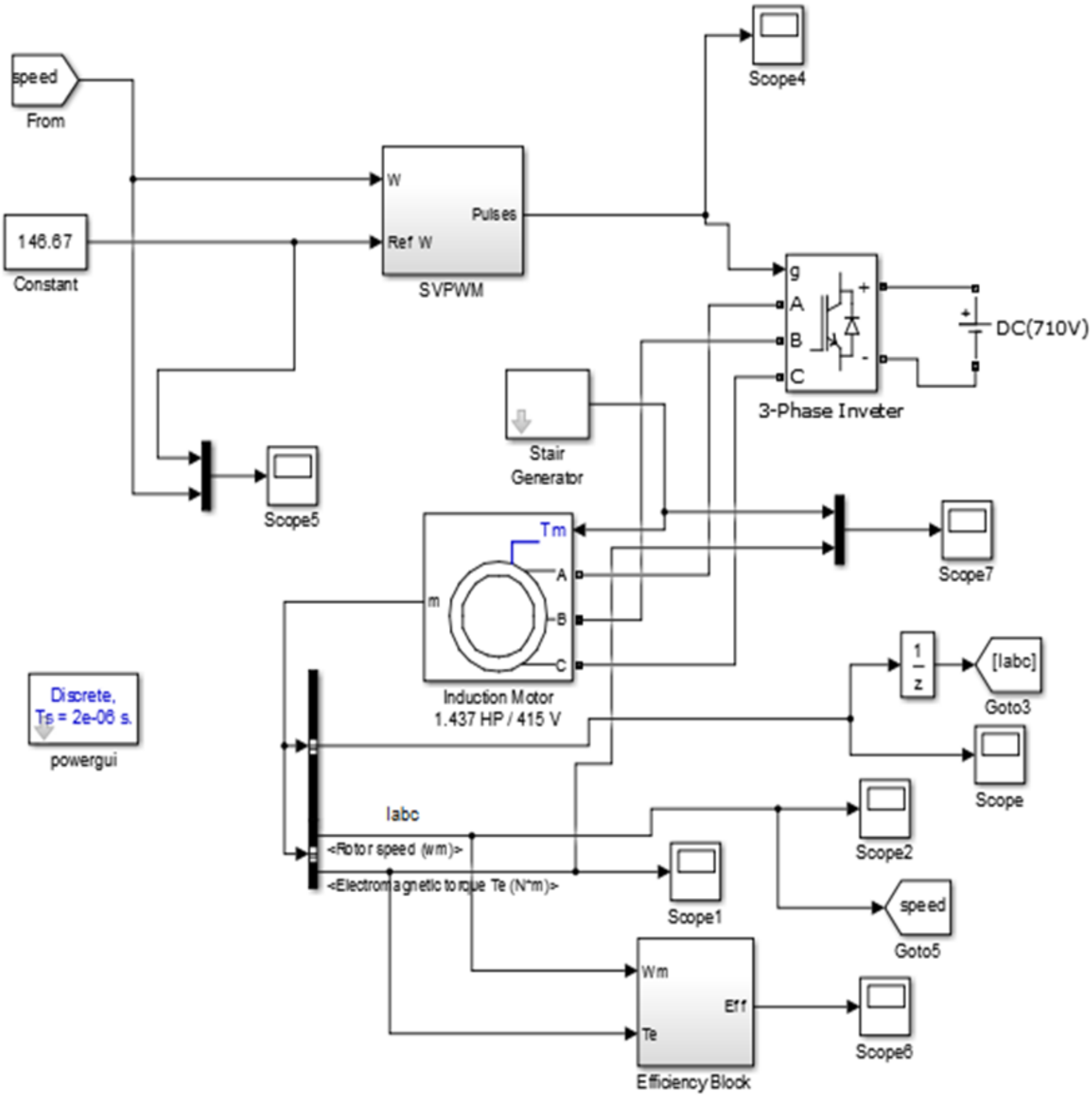

Figure A.4 A Simulink model for indirect vector control induction motor with PI controller using SVPWM Controller for generating pulses

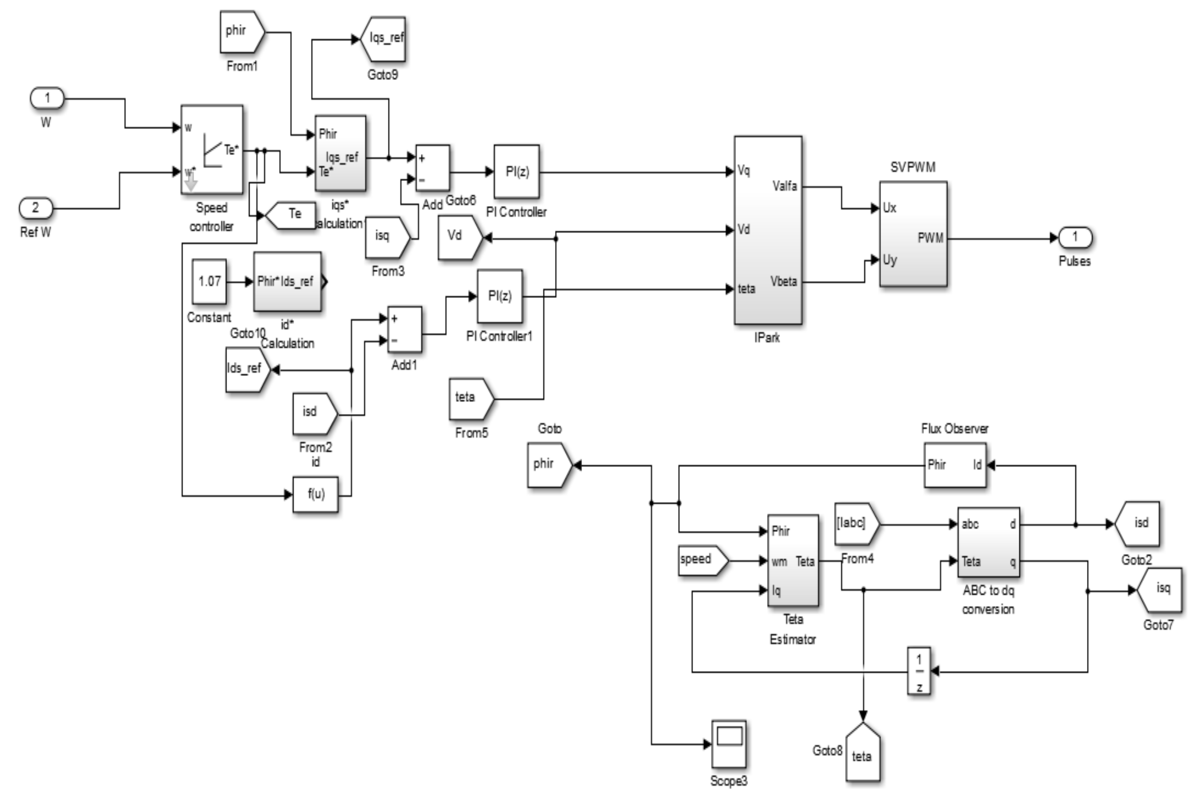

Figure A.5 Simulink model of indirect vector control for efficiency optimization using SVPWM